J Sci Comput (2018) 74:1115–1145
https://doi.org/10.1007/s10915-017-0484-x

Block-Centered Finite Difference Method for Simulating Compressible Wormhole Propagation

Xiaoli Li[1] · **Hongxing Rui**[1]

Received: 10 January 2017 / Revised: 1 June 2017 / Accepted: 9 June 2017 / Published online: 20 June 2017
© Springer Science+Business Media, LLC 2017

Abstract In this paper, the block-centered finite difference method is introduced and analyzed to solve the compressible wormhole propagation. The coupled analysis approach to deal with the fully coupling relation of multivariables is employed. By this, stability analysis and error estimates for the pressure, velocity, porosity, concentration and its flux in different discrete norms are established rigorously and carefully on non-uniform grids. Finally, some numerical experiments are presented to verify the theoretical analysis and effectiveness of the given scheme.

Keywords Block-centered finite difference · Compressible wormhole propagation · Non-uniform grids · Error estimates · Numerical experiments

Mathematics Subject Classification 65M06 · 65M12 · 65M15

1 Introduction

A wormhole is a phenomenon in which a worm-like hole is generated and propagated in the subsurface formations due to the injection of acids into a supercritical acid dissolution system. To enhance oil production rate, matrix acidization technique was introduced and applied widely. In this technique, we injected acid into matrix to dissolve the rocks, thus a channel called wormhole [1–6] is established. Usually such channel is formed with high porosities. Though this channel, we can easily push oil and gas components in the reservoir to the surface. It is crucial to point out that the advancement of the chemical reaction front does not propagate uniformly along the injection direction. Actually, the heterogeneity of

✉ Hongxing Rui
hxrui@sdu.edu.cn

Xiaoli Li
xiaolisdu@163.com

1 School of Mathematics, Shandong University, Jinan 250100, Shandong, China

porosity and permeability in the subsurface formations plays an significant role in promoting the non-uniformity of the chemical reaction front. All in all, the chemical reaction front tends to advance in certain directions more that other directions, thus a wormhole pattern is formed.

There are many numerical simulations for wormhole propagation due to its significant role in subsurface reservoir management. Zhao et al. [7] presented the theoretical and numerical analyses of chemical-dissolution front instability in fluid-saturated porous rocks by combining the finite element method and the finite difference method. In 2015, the new Darcy–Brinkman–Forchheimer framework was introduced to simulate the wormhole forming procedure by Wu et al. [3]. Besides, Kou et al. [1] developed a mixed finite element-based fully conservative methods to simulate the wormhole propagation. Recently, Li and Rui [8] have researched the characteristic block-centered finite difference method for simulating incompressible wormhole propagation.

Block-centered finite differences, sometimes called cell-centered finite differences, can be thought as the lowest order Raviart–Thomas mixed element method [9], with proper quadrature formulation. In [10], Wheeler presented the mixed finite elements for elliptic problems with tensor coefficients as cell-centered finite differences. And in 2012, a block-centered finite difference method for the Darcy–Forchheimer model was considered [11]. In [12–15] block-centered finite difference methods were developed. A parallel CGS block-centered finite difference method for a nonlinear time-fractional parabolic equation has been studied [16]. Recently, Li and Rui [17] applied this method to the nonlinear time-fractional parabolic equation. The applications of the block-centered finite difference methods enable us to approximate pressure, velocity, porosity, concentration and its flux in different discrete norms with second-order accuracy on non-uniform grids, which is the superconvergence. Also the block-centered finite difference methods can guarantee local mass conservation. Besides, the applications of the block-centered finite difference methods enable us to transfer the saddle point problem to symmetric positive definite problem.

As far as we know, there is no block-centered finite difference method for compressible wormhole propagation. Before analyzing the convergence of our block-centred finite difference method, we develop estimates of the mixed finite element method with quadrature applied to linear parabolic equations. Using these estimates, we obtain the superconvergence of the pressure, velocity, porosity, concentration and its flux in different discrete norms. In fact, in our proposed scheme, there are at least three issues in theoretical analysis for the compressible wormhole propagation: the first one is to estimate and bound the porosity which can change during time evolution, the second one is the complication resulted from the introduced auxiliary flux variable and the last one is the fully coupling relation of multi-variables. To resolve these issues, we introduce some usefully lemmas and consider the coupled analysis method. Recently, we have applied this method to the incompressible wormhole propagation in [8]. But for compressible wormhole propagation, due to the appearance of the term $\frac{\partial p}{\partial t}$ in the mass conservation equation, the same technique can not be used. Compared with the error analyses in [8], the error estimates in this paper is more complex which should be taken the time difference of approximate velocity and auxiliary flux into consideration. Moreover, stability results are proven rigorously and carefully which are not given in [8]. The error estimates are deduced rigorously and carefully in this paper, and we carry out some numerical experiments to verify the theoretical analysis and effectiveness of the given scheme.

The paper is organized as follows. In Sect. 2 we give the problem and some preliminaries. In Sect. 3 we present the block-centered finite difference algorithm. In Sect. 4 we demonstrate stability estimates for the discrete scheme. In Sect. 5 we demonstrate error analysis for the discrete scheme. In Sect. 6 some numerical experiments are carried out to verify the theoretical analysis and effectiveness of the given scheme.

Through out the paper we use C, with or without subscript, to denote a positive constant, which could have different values at different appearances.

2 The Problem and Some Preliminaries

In this paper, we consider the usual differential system used to describe compressible wormhole propagation [1]

$$\begin{cases} \gamma \dfrac{\partial p}{\partial t} + \dfrac{\partial \phi}{\partial t} + \nabla \cdot \mathbf{u} = f, \quad \mathbf{x} \in \Omega,\ t \in J, & (1) \\ \mathbf{u} = -\dfrac{K(\phi)}{\mu} \nabla p, \quad \mathbf{x} \in \Omega,\ t \in J, & (2) \\ \dfrac{\partial (\phi c_f)}{\partial t} + \nabla \cdot (\mathbf{u} c_f) - \nabla \cdot (\phi \mathbf{D}\, \nabla c_f) = k_c a_v (c_s - c_f) + f_P c_f + f_I c_I, & (3) \\ \dfrac{\partial \phi}{\partial t} = \dfrac{\alpha k_c a_v (c_f - c_s)}{\rho_s}, \quad \mathbf{x} \in \Omega,\ t \in J, & (4) \end{cases}$$

where Ω is a rectangular domain in $\mathbb{R}^2$. $J = (0, \hat{T}]$, and $\hat{T}$ denotes the final time. p is the pressure, μ is the fluid viscosity, $\mathbf{u}$ is the Darcy velocity of the fluid, $f = f_I + f_P$, f_P and f_I are production and injection rates respectively. γ is a pseudo-compressibility parameter that results in slight change of the density of the fluid phase in the dissolution process. c_f is the cup-mixing concentration of the acid in the fluid phase. c_I is the injected concentration. The diffusion coefficient $\mathbf{D}$ is shown as

$$\mathbf{D}(\mathbf{x}, \mathbf{u}) = d_m \mathbf{I} + \alpha_l |\mathbf{u}| \mathbf{E} + \alpha_t |\mathbf{u}| \mathbf{E}^{\perp}, \tag{5}$$

where $\mathbf{E}(\mathbf{u}) = [u_i u_j / |\mathbf{u}|^2]$ is a 2×2 matrix representing projection along the velocity vector and $\mathbf{E}^{\perp}(\mathbf{u})$ its orthogonal complement. d_m is the molecular diffusivity, the diffusion coefficient α_l measures the dispersion in the direction of flow and α_t that transverse to the flow.

k_c is the local mass-transfer coefficient, a_v is the interfacial area available for reaction per unit volume of the medium. The variable c_s is the concentration of the acid at the fluid-solid interface, and the relationship between c_f and c_s can be described as follows.

$$c_s = \frac{c_f}{1 + k_s / k_c}, \tag{6}$$

where k_s is the surface reaction rate constant. The first term in the right hand side of Eq. (3) represents the transfer of acid species from the fluid phase to the fluid-solid interface [2]. ϕ and K are the porosity and permeability of the rock respectively, the relationship between the permeability and the porosity is established by the Carman–Kozeny correlation [18]

$$\frac{K}{K_0} = \frac{\phi}{\phi_0} \left(\frac{\phi (1 - \phi_0)}{\phi_0 (1 - \phi)} \right)^2, \tag{7}$$

where ϕ_0 and K_0 are the initial porosity and permeability of the rock respectively. In Eq. (4), α is the dissolving power of the acid and ρ_s is the density of the solid phase. Using porosity and permeability, a_v is shown as

$$\frac{a_v}{a_0} = \frac{\phi}{\phi_0} \sqrt{\frac{K_0 \phi}{K \phi_0}}, \tag{8}$$

where a_0 is the initial interfacial area.
The boundary and initial conditions are as follows.

$$\begin{cases} \mathbf{u}\cdot\mathbf{n}=0,\ \phi\mathbf{D}\nabla c_f\cdot\mathbf{n}=0, & \mathbf{x}\in\partial\Omega,\ t\in J,\\ p(\mathbf{x},0)=p_0(\mathbf{x}), & \mathbf{x}\in\Omega,\\ c_f(\mathbf{x},0)=c_{f0}(\mathbf{x}), & \mathbf{x}\in\Omega,\\ \phi(\mathbf{x},0)=\phi_0(\mathbf{x}), & \mathbf{x}\in\Omega, \end{cases} \tag{9}$$

where $\mathbf{n}$ is the unit outward normal vector of the domain Ω. For the physical quantities, we assume that $0\le c_{f0}\le 1$ and $0\le c_I\le 1$.

Let $N>0$ be a positive integer. Set

$$\triangle t=\hat{T}/N,\quad t_n=n\triangle t,\quad for\ \ n\le N.$$

Let $L^m(\Omega)$ be the standard Banach space with norm

$$\|v\|_{L^m(\Omega)}=\left(\int_\Omega |v|^m d\Omega\right)^{1/m}.$$

For simplicity, let

$$(f,g)=(f,g)_{L^2(\Omega)}=\int_\Omega fgd\Omega$$

denote the $L^2(\Omega)$ inner product, $\|v\|_\infty=\|v\|_{L^\infty(\Omega)}$. And $W_p^k(\Omega)$ be the standard Sobolev space

$$W_p^k(\Omega)=\{g:\ \|g\|_{W_p^k(\Omega)}<\infty\},$$

where

$$\|g\|_{W_p^k(\Omega)}=\left(\sum_{|\alpha|\le k}\|D^\alpha g\|^p_{L^p(\Omega)}\right)^{1/p}. \tag{10}$$

Let $S=L^2(\Omega)$ and $\mathbf{V}=H(\Omega,div)=\{\boldsymbol{v}\in(L^2(\Omega))^2,\ \nabla\cdot\boldsymbol{v}\in L^2(\Omega)\}$. And $\mathbf{V}^0$ is denoted as the subspaces of $\mathbf{V}$ containing functions with normal traces equal to 0.

Let $\mathcal{T}_h$ be the quasi-uniform partition of Ω into rectangles in two dimensions with maximal mesh size h. The lowest-order Raviart–Thomas–Nédélec (RTN) space on rectangles [9,19] is considered. Thus, on an element $D\in\mathcal{T}_h$, we have

$$\mathbf{V}_h(D)=\left\{(\alpha_1x+\beta_1,\ \alpha_2y+\beta_2)^T:\ \alpha_i,\beta_i\in\mathbb{R},\ i=1,2\right\},$$
$$S_h(D)=\{\alpha:\ \alpha\in\mathbb{R}\},$$

and $\mathbf{V}_h^0$ is denoted as the subspaces of $\mathbf{V}_h$ containing functions with normal traces equal to 0.

Next the standard nodal basis is used, where the nodes are at the centers of the elements for S_h, and the nodes are at the midpoints of edges for $\mathbf{V}_h$. Moreover, the grid points are denoted by

$$(x_{i+1/2},y_{j+1/2}),\quad i=0,\ldots,N_x,\quad j=0,\ldots,N_y,$$

and the notations similar to those in [20] are used.

$$
\begin{aligned}
&x_i = \left(x_{i-\frac{1}{2}} + x_{i+\frac{1}{2}}\right)/2, \quad i = 1, \ldots, N_x,\\
&h_i^x = x_{i+\frac{1}{2}} - x_{i-\frac{1}{2}}, \quad i = 1, \ldots, N_x,\\
&h_{i+\frac{1}{2}}^x = x_{i+1} - x_i = \left(h_i^x + h_{i+1}^x\right)/2, \quad i = 1, \ldots, N_x - 1,\\
&y_j = \left(y_{j-\frac{1}{2}} + y_{j+\frac{1}{2}}\right)/2, \quad j = 1, \ldots, N_y,\\
&h_j^y = y_{j+\frac{1}{2}} - y_{j-\frac{1}{2}}, \quad j = 1, \ldots, N_y,\\
&h_{j+\frac{1}{2}}^y = y_{j+1} - y_j = \left(h_j^y + h_{j+1}^y\right)/2, \quad j = 1, \ldots, N_y,\\
&h = \max_{i,j}\left\{h_i^x, h_j^y\right\}.
\end{aligned}
$$

Let $g_{i,j}$, $g_{i+\frac{1}{2},j}$, $g_{i,j+\frac{1}{2}}$ denote $g(x_i, y_j)$, $g(x_{i+\frac{1}{2}}, y_j)$, $g(x_i, y_{j+\frac{1}{2}})$. Define the discrete inner products and norms as follows,

$$
\begin{aligned}
(f, g)_M &= \sum_{i=1}^{N_x}\sum_{j=1}^{N_y} h_i^x h_j^y f_{i,j} g_{i,j},\\
(f, g)_x &= \sum_{i=1}^{N_x-1}\sum_{j=1}^{N_y} h_{i+\frac{1}{2}}^x h_j^y f_{i+\frac{1}{2},j} g_{i+\frac{1}{2},j},\\
(f, g)_y &= \sum_{i=1}^{N_x}\sum_{j=1}^{N_y-1} h_i^x h_{j+\frac{1}{2}}^y f_{i,j+\frac{1}{2}} g_{i,j+\frac{1}{2}},\\
(\boldsymbol{v}, \boldsymbol{r})_{TM} &= (v^x, r^x)_x + (v^y, r^y)_y.
\end{aligned}
$$

For simplicity from now on we always omit the superscript n if the omission does not cause conflicts. Define

$$
\begin{aligned}
[d_x g]_{i+\frac{1}{2},j} &= \left(g_{i+1,j} - g_{i,j}\right)/h_{i+\frac{1}{2}}^x,\\
[d_y g]_{i,j+\frac{1}{2}} &= \left(g_{i,j+1} - g_{i,j}\right)/h_{j+\frac{1}{2}}^y,\\
[D_x g]_{i,j} &= \left(g_{i+\frac{1}{2},j} - g_{i-\frac{1}{2},j}\right)/h_i^x,\\
[D_y g]_{i,j} &= \left(g_{i,j+\frac{1}{2}} - g_{i,j-\frac{1}{2}}\right)/h_j^y,\\
[d_t g]_{i,j}^n &= \left(g_{i,j}^n - g_{i,j}^{n-1}\right)/\Delta t.
\end{aligned}
$$

Then we present some lemmas used in the following estimates.

Lemma 1 [20] *Let $q_{i,j}$, $w_{i+1/2,j}^x$ and $w_{i,j+1/2}^y$ be any values such that $w_{1/2,j}^x = w_{N_x+1/2,j}^x = w_{i,1/2}^y = w_{i,N_y+1/2}^y = 0$, then*

$$
\begin{aligned}
(q, D_x w^x)_M &= -(d_x q, w^x)_x,\\
(q, D_y w^y)_M &= -(d_y q, w^y)_y.
\end{aligned}
$$

For any $\boldsymbol{r} \in (H^2(\Omega))^2$, let $\hat{\boldsymbol{r}}$ denote the projection operator of $\boldsymbol{r}$ onto $\mathbf{V}_h$, that is

$$(\nabla \cdot \hat{\boldsymbol{r}}, w) = (\nabla \cdot \boldsymbol{r}, w), \quad \forall w \in S_h, \tag{11}$$

with approximation properties [21],

$$\|\boldsymbol{r} - \hat{\boldsymbol{r}}\| \le C\|\boldsymbol{r}\|_{W_2^1(\Omega)} h, \tag{12}$$

$$\|\nabla \cdot (\boldsymbol{r} - \hat{\boldsymbol{r}})\| \le C\|\nabla \cdot \boldsymbol{r}\|_{W_2^1(\Omega)} h. \tag{13}$$

Moreover, by the definition of $\hat{\boldsymbol{r}}$ and the midpoint rule of integration, the L^∞ norm of the projection is obtained by

$$\|\hat{\boldsymbol{r}} - \boldsymbol{r}\|_{L^\infty(\Omega)} \le Ch\|\boldsymbol{r}\|_{W_\infty^2(\Omega)}. \tag{14}$$

In Eq. (3), define $\boldsymbol{q} = -\phi \mathbf{D}(\mathbf{x})\nabla c_f$, we can get the estimates which is necessary for the derivative and analysis of our numerical scheme [22].

$$\|\hat{\boldsymbol{u}}^n - \boldsymbol{u}^n\|_{TM} \le Ch^2, \tag{15}$$

$$\|\hat{\boldsymbol{q}}^n - \boldsymbol{q}^n\|_{TM} \le Ch^2. \tag{16}$$

Next we define an interpolant operator which is similar to that in [21]. Define $\Pi_h p$ from the values of $p_{i,j}$ for $i = 1, 2, \ldots, N_x$ and $j = 1, 2, \ldots, N_y$ as follows. For points (x, y), assuming $x \in [x_i, x_{i+1}]$, $y \in [y_j, y_{j+1}]$, then, $\Pi_h p(x, y)$ can be evaluated by

$$\begin{aligned}\Pi_h p(x, y) = &\left(p_{i,j}\left(\frac{x_{i+1} - x}{x_{i+1} - x_i}\right) + p_{i+1,j}\left(\frac{x - x_i}{x_{i+1} - x_i}\right)\right)\left(\frac{y_{j+1} - y}{y_{j+1} - y_j}\right)\\ &+ \left(p_{i,j+1}\left(\frac{x_{i+1} - x}{x_{i+1} - x_i}\right) + p_{i+1,j+1}\left(\frac{x - x_i}{x_{i+1} - x_i}\right)\right)\left(\frac{y - y_j}{y_{j+1} - y_j}\right).\end{aligned}$$

For $j = 1, 2 \ldots N_y$, we set

$$\Pi_h p(x_{1/2}, y_j) = \frac{\left(2h_1^x + h_2^x\right) p_{1j} - h_1^x p_{2j}}{h_1^x + h_2^x}.$$

This is a two-point extrapolation, and by Taylor's expansion, we can obtain that

$$|(\Pi_h p - p)(x_{1/2}, y_j)| = O(h^2).$$

For points (x, y), assuming $x \in [x_{1/2}, x_1]$, $y \in [y_j, y_{j+1}]$, then, $\Pi_h p(x, y)$ can be evaluated as the bilinear interpolant between $p_{1,j}$, $p_{1,j+1}$, $\Pi_h p(x_{1/2}, y_j)$, and $\Pi_h p(x_{1/2}, y_{j+1})$. And for these points, we can obtain that $|\Pi_h p - p| \le Ch^2$ by interpolation theory. Moreover, for points (x, y), such that $x \in [x_{N_x}, x_{N_x+1/2}]$, $y \in [y_j, y_{j+1}]$ as well as points (x, y), where $x \in [x_i, x_{i+1}]$, $y \in [y_{1/2}, y_1]$ or $x \in [x_i, x_{i+1}]$, $y \in [y_{N_y}, y_{N_y+1/2}]$, we can define $\Pi_h p$ similarly. Lastly, we can define $\Pi_h p(x_{1/2}, y_{1/2})$ using three-point extrapolation:

$$\begin{aligned}\Pi_h p(x_{1/2}, y_{1/2}) &= \Pi_h p(x_1, y_{1/2}) + \Pi_h p(x_{1/2}, y_1) - p_{1,1}\\ &= p_{1,1/2} + p_{1/2,1} - p_{1,1} + Ch^2.\end{aligned}$$

We can easily obtain that $|(\Pi_h p - p)(x_{1/2}, y_{1/2})| \le Ch^2$ by Taylor's theorem. Hence, for points (x, y), assuming $x \in [x_{1/2}, x_1]$, $y \in [y_{1/2}, y_1]$, $\Pi_h p(x, y)$ can be evaluated as the bilinear interpolant between $p_{1,1}$, $\Pi_h p_{1/2,1}$, $\Pi_h p_{1,1/2}$, and $\Pi_h p_{1/2,1/2}$. We can define $\Pi_h p_{1/2,N_y+1/2}$, $\Pi_h p_{N_x+1/2,1/2}$, $\Pi_h p_{N_x+1/2,N_y+1/2}$ similarly. And in the other three corner regions, the same approximations can be obtained. Thus we can get the following lemma.

Lemma 2 [21] *Suppose p is twice differentiable in space, then we have the estimate that*

$$||\Pi_h p - p||_\infty \le Ch^2.$$

Lastly, we make the following assumptions which are similar to Kou et al. in [1].

(H1) $p,\ c_f \in W^2_\infty(0, T; W^4_\infty(\Omega))$.
(H2) $D_{ll}(\mathbf{x}) \in W^3_\infty(\Omega)$, $\phi \in C^1(0, T; C^2(\Omega))$.
(H3) There exist four positive constants K_*, K^*, D_* and D^* such that

$$K_* \le K(\mathbf{x}, \phi) \le K^*, \quad D_* \le D_{ll}(\mathbf{x}) \le D^*, \quad for\ \mathbf{x} \in \Omega,\ \phi \in \mathbb{R},\ l = 1, 2. \tag{17}$$

(H4) $K(\phi)^{-1}$ is uniformly Lipschitz function of ϕ.
(H5) $\gamma,\ \alpha,\ \rho_s,\ \mu,\ k_c$ and k_s are all given positive constants, and $0 < \phi_{0*} \le \phi_0 \le \phi_0^* < 1$, $0 \le a_{0*} \le a_0 \le a_0^*$.

3 A Block-Centered Finite Difference Algorithm

In this section, in order to solve the nonlinear system (1)–(8) efficiently, the block-centered finite difference algorithm is considered.

Using Eqs. (6)–(8), nonlinear system (1)–(4) can be transformed into

$$\begin{cases} \gamma \dfrac{\partial p}{\partial t} + \dfrac{\partial \phi}{\partial t} + \nabla \cdot \mathbf{u} = f, & (18)\\ \mathbf{u} = -\dfrac{K(\phi)}{\mu}\nabla p, & (19)\\ \phi \dfrac{\partial c_f}{\partial t} - \gamma c_f \dfrac{\partial p}{\partial t} - (\phi \mathbf{D})^{-1}\mathbf{u}\cdot\mathbf{q} + \nabla\cdot\mathbf{q} + f_I c_f + \dfrac{k_c k_s}{k_c + k_s} a_v c_f = f_I c_I, & (20)\\ \dfrac{\partial \phi}{\partial t} = \dfrac{r_\phi(1-\phi)}{1-\phi_0} c_f, & (21) \end{cases}$$

where $r_\phi = \dfrac{\alpha a_0 k_c k_s}{\rho_s(k_c + k_s)}$, and taking notice of assumption $(H5)$, we obtain $0 \le r_{\phi *} \le r_\phi \le r_\phi^*$.

To obtain superconvergence, we shall also consider only molecular diffusion [23,24] in the following. Denoted by $\{Z^n, \boldsymbol{W}^n, \Psi^n, \boldsymbol{Q}^n\}_{n=0}^N$, the block-centered finite difference approximations to $\{p^n, \boldsymbol{u}^n, c_f^n, \boldsymbol{q}^n\}_{n=0}^N$ respectively are as follows, where $Z^n, \Psi^n \in S_h$, $\boldsymbol{W}^n, \boldsymbol{Q}^n \in \mathbf{V}_h^0$.

$$\begin{cases} (\gamma d_t Z^n + d_t \Theta^n + \nabla\cdot\boldsymbol{W}^n, w) = (f^n, w), \quad \forall w \in S_h, & (22)\\ \left(\dfrac{\mu}{K(\Pi_h\Theta^n)}\boldsymbol{W}^n, \boldsymbol{v}\right)_{TM} = (Z^n, \nabla\cdot\boldsymbol{v}), \quad \forall \boldsymbol{v} \in \mathbf{V}_h^0, & (23)\\ (\Theta^n d_t\Psi^n, w) - (\gamma\overline{\Psi}^{n-1} d_t Z^n, w) - \big(((\Theta^n\mathbf{D})^{-1}\Pi_h\mathbf{W}^n\cdot\Pi_h\mathbf{Q}^n, w\big) + \big(f_I^n\Psi^n, w\big) & \\ \quad + (\nabla\cdot\boldsymbol{Q}^n, w) + \dfrac{k_c k_s}{k_c + k_s}\big(a_v(\Theta^n)\Psi^n, w\big) = \big(f_I^n c_I^n, w\big), \quad \forall w \in S_h, & (24)\\ ((\Pi_h\Theta^n\mathbf{D})^{-1}\boldsymbol{Q}^n, \boldsymbol{v})_{TM} = (\Psi^n, \nabla\cdot\boldsymbol{v}), \quad \forall\boldsymbol{v} \in \mathbf{V}_h^0. & (25) \end{cases}$$

For the calculation of the discrete porosity Θ, we use the following scheme.

$$[d_t\Theta]^n_{i,j} = \frac{r^n_{\phi,i,j}\left(1-\Theta^n_{i,j}\right)}{1-\phi_{0,i,j}}\overline{\Psi}^{n-1}_{i,j}, \tag{26}$$

where $\overline{\Psi}^{n-1} = \max\left\{0, \min\{\Psi^{n-1}, 1\}\right\}$.

Set the boundary and initial approximations as follows.

$$\begin{cases} W^{x,n}_{1/2,j} = W^{x,n}_{N_x+1/2,j} = 0, & 1 \le j \le N_y, \\ W^{y,n}_{i,1/2} = W^{y,n}_{i,N_y+1/2} = 0, & 1 \le i \le N_x, \\ Q^{x,n}_{1/2,j} = Q^{x,n}_{N_x+1/2,j} = 0, & 1 \le j \le N_y, \\ Q^{y,n}_{i,1/2} = Q^{y,n}_{i,N_y+1/2} = 0, & 1 \le i \le N_x, \\ Z^0_{i,j} = p_{0,i,j},\ 1 \le i \le N_x, & 1 \le j \le N_y, \\ \Psi^0_{i,j} = c_{f0,i,j},\ 1 \le i \le N_x, & 1 \le j \le N_y, \\ \Theta^0_{i,j} = \phi_{0,i,j},\ 1 \le i \le N_x, & 1 \le j \le N_y. \end{cases} \tag{27}$$

The difference method will consist of three parts: firstly, if the approximate concentration $\Psi^{n-1}_{i,j}$ and porosity $\Theta^{n-1}_{i,j}$, $n = 1, \ldots, N$ are known, Eq. (26) will be used to obtain a new porosity $\Theta^n_{i,j}$; Secondly, by difference scheme (22)–(23), an approximation $Z^n_{i,j}$ to the pressure will be calculated using $\Theta^n_{i,j}$, and the approximate velocity $W^{x,n}_{i+1/2,j}$ and $W^{y,n}_{i,j+1/2}$ will be evaluated; Finally, a new concentration $\Psi^n_{i,j}$ will be calculated using $W^{x,n}_{i+1/2,j}$, $W^{y,n}_{i,j+1/2}$, $d_t Z^n_{i,j}$ and $\Theta^n_{i,j}$, then we get the approximations $Q^{x,n}_{i+1/2,j}$ and $Q^{y,n}_{i,j+1/2}$. It is easy to see that at each time level, the difference scheme has an explicit solution or is a linear system with strictly diagonally dominant coefficient matrix, thus the approximate solutions exist uniquely.

Remark 1 For the case that $\mathbf{D}$ is defined by Eq. (5), the block-centered finite difference approximations have a little difference in Eqs. (24) and (25). Here we define $\tilde{\boldsymbol{q}} = -\nabla c_f$, $\boldsymbol{q} = \phi\mathbf{D}(\mathbf{u})\tilde{\boldsymbol{q}}$, then denoted by $\{\Psi^n, \widetilde{\boldsymbol{Q}}^n, \boldsymbol{Q}^n\}_{n=0}^N$, the block-centered finite difference approximations to $\{c^n_f, \tilde{\boldsymbol{q}}^n, \boldsymbol{q}^n\}_{n=0}^N$ respectively are as follows:

$$\begin{aligned} &\left(\Theta^n d_t\Psi^n, w\right) - \left(\gamma\overline{\Psi}^{n-1} d_t Z^n, w\right) - \left(\Pi_h\mathbf{W}^n\cdot\Pi_h\widetilde{\mathbf{Q}}^n, w\right) + \left(f^n_I\Psi^n, w\right) \\ &\quad + (\nabla\cdot\boldsymbol{Q}^n, w) + \frac{k_c k_s}{k_c+k_s}\left(a_v(\Theta^n)\Psi^n, w\right) = \left(f^n_I c^n_I, w\right), \quad \forall w \in S_h, \end{aligned} \tag{28}$$

$$\left(\widetilde{\boldsymbol{Q}}^n, \boldsymbol{v}\right)_{TM} = \left(\Psi^n, \nabla\cdot\boldsymbol{v}\right), \quad \forall\boldsymbol{v} \in \mathbf{V}^0_h, \tag{29}$$

$$\left(\boldsymbol{Q}^n, \boldsymbol{v}\right)_{TM} = (\Pi_h\Theta^n\mathbf{D}(\Pi_h\mathbf{W}^n)\widetilde{\mathbf{Q}}^n, \boldsymbol{v})_T, \quad \forall\boldsymbol{v} \in \mathbf{V}^0_h, \tag{30}$$

where $(\cdot,\cdot)_T$ is the trapezoidal rule defined by

$$\begin{aligned} (\mathbf{f},\mathbf{g})_T = &\sum_{i=1}^{N_x-1}\sum_{j=1}^{N_y} h^x_{i+1/2}h^y_j\cdot\frac{1}{2}\left(f^x_{i+1/2,j-1/2}g^x_{i+1/2,j-1/2} + f^x_{i+1/2,j+1/2}g^x_{i+1/2,j+1/2}\right) \\ &+ \sum_{i=1}^{N_x}\sum_{j=1}^{N_y-1} h^x_i h^y_{j+1/2}\cdot\frac{1}{2}\left(f^y_{i-1/2,j+1/2}g^y_{i-1/2,j+1/2} + f^y_{i+1/2,j+1/2}g^y_{i+1/2,j+1/2}\right). \end{aligned}$$

Here we use the trapezoidal rule to maintain symmetry in the case that $\mathbf{D}$ is not diagonal, which is similar to that in [10].

4 Stability Analysis for the Discrete Scheme

In this section, we will give the analysis of stability for the scheme (22)–(26).

For the purpose of theoretical analysis, we first analysis a priori bounds for the discrete solution Θ.

Theorem 3 *Assuming that* $0 < \phi_{0*} \leq \phi_0 \leq \phi_0^* < 1$, *then the discrete porosity* $\Theta_{i,j}^n$ *is bounded, i.e.,*

$$\phi_{0*} \leq \Theta_{i,j}^n < 1, \ \ 1 \leq i \leq N_x, \ 1 \leq j \leq N_y, \ n \leq N.$$

Proof The proof is given by induction. It is trivial that $\phi_{0*} \leq \Theta_{i,j}^0 < 1$. Suppose that

$$\phi_{0*} \leq \Theta_{i,j}^{k-1} < 1, \ k \leq N,$$

next we prove that $\Theta_{i,j}^k$ also does.

For simplicity, set $\beta^{k-1} = \dfrac{r_\phi \overline{\Psi}^{k-1}}{1-\phi_0}\Delta t$, where $\overline{\Psi}^{n-1} = \max\left\{0, \min\{\Psi^{n-1}, 1\}\right\}$. Then Eq. (26) can be transformed into the following.

$$\Theta_{i,j}^k = \frac{\beta_{i,j}^{k-1}}{1+\beta_{i,j}^{k-1}} + \frac{\Theta_{i,j}^{k-1}}{1+\beta_{i,j}^{k-1}}. \tag{31}$$

By Eq. (31), we can easily obtain that $\Theta_{i,j}^k < 1$. Equation (26) can also be calculated as

$$\Theta_{i,j}^k - \Theta_{i,j}^{k-1} = \beta_{i,j}^{k-1}(1-\Theta_{i,j}^k), \tag{32}$$

thus we have that $\Theta_{i,j}^k > \Theta_{i,j}^{k-1}$. Then the proof ends. □

Theorem 4 *The approximate solutions of* (22)–(25) *satisfy*

$$\|Z^m\|_M^2 + \|\frac{\mu}{K(\Pi_h\Theta^m)}\boldsymbol{W}^m\|_{TM}^2 \leq C\sum_{n=1}^m \Delta t\|f^n\|_M^2 + C\|p_0\|_M^2 + C\|\boldsymbol{u}_0\|_{TM}^2 + Cr_\phi^{*2}, \ \ m \leq N, \tag{33}$$

$$\|\Psi^m\|_M^2 + \|\boldsymbol{Q}^m\|_{TM}^2 + \sum_{n=1}^m \Delta t\|\boldsymbol{Q}^n\|_{TM}^2 \leq C\left(\|\boldsymbol{q}_0\|_{TM}^2 + \|\boldsymbol{u}_0\|_{TM}^2 + \|c_{f0}\|_M^2 + r_\phi^{*2}\right) + C\sum_{n=1}^m \Delta t\left(\|f_I^n c_I^n\|_M^2 + \|f^n\|_M^2\right), \ \ m \leq N. \tag{34}$$

Proof Taking notice of Eq. (23), we have

$$\left(d_t\left(\frac{\mu}{K(\Pi_h\Theta^n)}\boldsymbol{W}^n\right), \boldsymbol{v}\right)_{TM} = \left(d_t Z^n, \nabla\cdot\boldsymbol{v}\right), \quad \forall \boldsymbol{v} \in \mathbf{V}_h^0. \tag{35}$$

Setting $w = d_t Z^n$ and $\boldsymbol{v} = \boldsymbol{W}^n$ in Eqs. (22) and (35) respectively, we have

$$\gamma\|d_t Z^n\|_M^2 + \left(\nabla\cdot\boldsymbol{W}^n, d_t Z^n\right) = \left(f^n, d_t Z^n\right) - \left(d_t\Theta^n, d_t Z^n\right), \tag{36}$$

and

$$\left(d_t\left(\frac{\mu}{K\left(\Pi_h\Theta^n\right)}\boldsymbol{W}^n\right),\boldsymbol{W}^n\right)_{TM}=(d_tZ^n,\nabla\cdot\boldsymbol{W}^n). \tag{37}$$

Then using Cauchy–Schwarz inequality, we have

$$\begin{aligned}&\gamma\|d_tZ^n\|_M^2+\left(d_t\left(\frac{\mu}{K(\Pi_h\Theta^n)}\boldsymbol{W}^n\right),\boldsymbol{W}^n\right)_{TM}\\&\quad\le C\|f^n\|_M^2+C\|d_t\Theta^n\|_M^2+\frac{\gamma}{2}\|d_tZ^n\|_M^2.\end{aligned} \tag{38}$$

The second term in the left hand side of Eq. (38) can be estimated by

$$\begin{aligned}&\left(d_t\left(\frac{\mu}{K(\Pi_h\Theta^n)}\boldsymbol{W}^n\right),\boldsymbol{W}^n\right)_{TM}\\&=\frac{1}{2}d_t\|\frac{\mu}{K(\Pi_h\Theta^n)}\boldsymbol{W}^n\|_{TM}^2+\frac{\Delta t}{2}\frac{\mu}{K(\Pi_h\Theta^{n-1})}\|d_t\boldsymbol{W}^n\|_{TM}^2\\&\quad+\frac{1}{2}\left(d_t\left(\frac{\mu}{K(\Pi_h\Theta^n)}\right)\boldsymbol{W}^n,\boldsymbol{W}^n\right)_{TM}.\end{aligned} \tag{39}$$

Noting Theorem 3, we can easily obtain

$$|d_t\Theta^n_{i,j}|\le\frac{1-\phi_{0*}}{1-\phi_0^*}r_\phi^*\le Cr_\phi^*. \tag{40}$$

Combining Eq. (38) with Eqs. (39) and (40), we have

$$\begin{aligned}&\frac{\gamma}{2}\|d_tZ^n\|_M^2+\frac{1}{2}d_t\|\frac{\mu}{K(\Pi_h\Theta^n)}\boldsymbol{W}^n\|_{TM}^2\\&\quad\le C\|f^n\|_M^2+C\|\boldsymbol{W}^n\|_{TM}^2+Cr_\phi^{*2}.\end{aligned} \tag{41}$$

Multiplying Eq. (41) by $2\Delta t$, summing for n from 1 to m, $m\le N$ and applying Gronwall's inequality, we have

$$\begin{aligned}&\gamma\sum_{n=1}^m\Delta t\|d_tZ^n\|_M^2+\|\frac{\mu}{K(\Pi_h\Theta^m)}\boldsymbol{W}^m\|_{TM}^2\\&\quad\le C\sum_{n=1}^m\Delta t\|f^n\|_M^2+C\|\boldsymbol{u}_0\|_{TM}^2+Cr_\phi^{*2}.\end{aligned} \tag{42}$$

Taking notice of that

$$Z^n_{i,j}=Z^0_{i,j}+\Delta t\sum_{k=1}^n d_tZ^k_{i,j},\ 1\le i\le N_x,\ 1\le j\le N_y,\ 1\le n\le N,$$

and using Cauchy–Schwarz inequality, we obtain that

$$\begin{aligned}\left(Z^n_{i,j}\right)^2&\le2\left(Z^0_{i,j}\right)^2+2\left(\Delta t\sum_{k=1}^n d_tZ^k_{i,j}\right)^2\\&\le2\left(Z^0_{i,j}\right)^2+2T\Delta t\sum_{k=1}^n\left(d_tZ^k_{i,j}\right)^2,\ 1\le i\le N_x,\ 1\le j\le N_y,\ 1\le n\le N.\end{aligned} \tag{43}$$

Then multiplying both sides of Eq. (43) by $h_i k_j$, and making summation on i, j for $1 \le i \le N_x,\ 1 \le j \le N_y$, we have that

$$\|Z^n\|_m^2 \le 2\|Z^0\|_m^2 + 2T\Delta t \sum_{k=1}^{n} \|d_t Z^k\|_m^2. \tag{44}$$

Thus we have

$$\begin{aligned} &\|Z^m\|_M^2 + \left\| \frac{\mu}{K(\Pi_h \Theta^m)} \boldsymbol{W}^m \right\|_{TM}^2 \\ &\quad \le C \sum_{n=1}^{m} \Delta t \|f^n\|_M^2 + C\|p_0\|_M^2 + C\|\boldsymbol{u}_0\|_{TM}^2 + C r_\phi^{*2}. \end{aligned} \tag{45}$$

We now turn to prove Eq. (34). From Eq. (25), we have

$$(d_t((\Pi_h \Theta^n \mathbf{D})^{-1} \boldsymbol{Q}^n), \boldsymbol{v})_{TM} = (d_t \Psi^n, \nabla \cdot \boldsymbol{v}), \quad \forall \boldsymbol{v} \in \mathbf{V}_h^0. \tag{46}$$

Setting $w = d_t \Psi^n$ and $\boldsymbol{v} = \mathbf{Q}^n$ in Eqs. (24) and (46) leads to

$$\begin{aligned} &(\Theta^n d_t \Psi^n, d_t \Psi^n) + (\nabla \cdot \boldsymbol{Q}^n, d_t \Psi^n) \\ &\quad = (f_I^n c_I^n, d_t \Psi^n) + (\gamma \overline{\Psi}^{n-1} d_t Z^n, d_t \Psi^n) + \left((\Theta^n \mathbf{D})^{-1} \Pi_h \mathbf{W}^n \cdot \Pi_h \mathbf{Q}^n, d_t \Psi^n\right) \\ &\quad\quad - (f_I^n \Psi^n, d_t \Psi^n) - \frac{k_c k_s}{k_c + k_s} (a_v(\Theta^n) \Psi^n, d_t \Psi^n), \end{aligned} \tag{47}$$

and

$$(d_t((\Pi_h \Theta^n \mathbf{D})^{-1} \boldsymbol{Q}^n), \mathbf{Q}^n)_{TM} = (d_t \Psi^n, \nabla \cdot \mathbf{Q}^n). \tag{48}$$

Combining Eq. (47) with Eq. (48) and using Cauchy–Schwarz inequality, we have

$$\begin{aligned} &\phi_{0*} \|d_t \Psi^n\|_M^2 + (d_t((\Pi_h \Theta^n \mathbf{D})^{-1} \boldsymbol{Q}^n), \mathbf{Q}^n)_{TM} \\ &\quad \le C\|f_I^n c_I^n\|_M^2 + C\|d_t Z^n\|_M^2 + C\|\Psi^n\|_M^2 + \frac{\phi_{0*}}{4} \|d_t \Psi^n\|_M^2 \\ &\quad\quad + \left((\Theta^n \mathbf{D})^{-1} \Pi_h \mathbf{W}^n \cdot \Pi_h \mathbf{Q}^n, d_t \Psi^n\right). \end{aligned} \tag{49}$$

The second term in the left hand side of Eq. (49) can be estimated by

$$\begin{aligned} &\left(d_t((\Pi_h \Theta^n \mathbf{D})^{-1} \boldsymbol{Q}^n), \boldsymbol{Q}^n\right)_{TM} \\ &\quad = \frac{1}{2} d_t \|(\Pi_h \Theta^n \mathbf{D})^{-1} \boldsymbol{Q}^n\|_{TM}^2 + \frac{\Delta t}{2} (\Pi_h \Theta^{n-1} \mathbf{D})^{-1} \|d_t \boldsymbol{Q}^n\|_{TM}^2 \\ &\quad\quad + \frac{1}{2} \left(d_t((\Pi_h \Theta^n \mathbf{D})^{-1}) \boldsymbol{Q}^n, \boldsymbol{Q}^n\right)_{TM}. \end{aligned} \tag{50}$$

To estimate the last term in the right hand side of Eq. (49), we give the following hypothesis first. Suppose that there exists a positive constant C^* such that

$$\|\Pi_h \mathbf{W}^n\|_\infty \le C^*. \tag{51}$$

Then we have

$$\begin{aligned} &\frac{\phi_{0*}}{2} \|d_t \Psi^n\|_M^2 + \frac{1}{2} d_t \|(\Pi_h \Theta^n \mathbf{D})^{-1} \boldsymbol{Q}^n\|_{TM}^2 \\ &\quad \le C\|f_I^n c_I^n\|_M^2 + C\|d_t Z^n\|_M^2 + C\|\Psi^n\|_M^2 + C\|\mathbf{Q}^n\|_{TM}^2. \end{aligned} \tag{52}$$

Multiplying Eq. (52) by $2\Delta t$, and summing for n from 1 to m, $m \leq N$, we have

$$\begin{aligned}
&\phi_{0*}\sum_{n=1}^{m}\Delta t\|d_t\Psi^n\|_M^2 + \|(\Pi_h\Theta^m\mathbf{D})^{-1}\boldsymbol{Q}^m\|_{TM}^2\\
&\quad\leq C\sum_{n=1}^{m}\Delta t\|f_I^n c_I^n\|_M^2 + C\sum_{n=1}^{m}\Delta t\|d_t Z^n\|_M^2 + C\sum_{n=1}^{m}\Delta t\|\Psi^n\|_M^2\\
&\qquad + C\sum_{n=1}^{m}\Delta t\|\mathbf{Q}^n\|_{TM}^2 + C\|(\Pi_h\Theta^0\mathbf{D})^{-1}\boldsymbol{q}_0\|_{TM}^2
\end{aligned}\tag{53}$$

Next we give the estimates for $\|\Psi^n\|_M^2$. Setting $w = \Psi^n$ and $\boldsymbol{v} = \boldsymbol{Q}^n$ in Eqs. (24) and (25) respectively, we have

$$\begin{aligned}
&\left(\Theta^n d_t\Psi^n, \Psi^n\right) + \left(\nabla\cdot\boldsymbol{Q}^n, \Psi^n\right)\\
&= \left(f_I^n c_I^n, \Psi^n\right) + \left(\gamma\overline{\Psi}^{n-1}d_t Z^n, \Psi^n\right) + \left((\Theta^n\mathbf{D})^{-1}\Pi_h\mathbf{W}^n\cdot\Pi_h\mathbf{Q}^n, \Psi^n\right)\\
&\quad - \left(f_I^n\Psi^n, \Psi^n\right) - \frac{k_c k_s}{k_c+k_s}\left(a_v(\Theta^n)\Psi^n, \Psi^n\right),
\end{aligned}\tag{54}$$

and

$$((\Pi_h\Theta^n\mathbf{D})^{-1}\boldsymbol{Q}^n, \boldsymbol{Q}^n)_{TM} = (\Psi^n, \nabla\cdot\boldsymbol{Q}^n).\tag{55}$$

By the similar estimates with the above equations, we can easily obtain

$$\begin{aligned}
&\|\Psi^m\|_M^2 + C\sum_{n=1}^{m}\Delta t\|\boldsymbol{Q}^n\|_{TM}^2\\
&\quad\leq C\sum_{n=1}^{m}\Delta t\|f_I^n c_I^n\|_M^2 + C\sum_{n=1}^{m}\Delta t\|d_t Z^n\|_M^2\\
&\qquad + C\sum_{n=1}^{m}\Delta t\|\Psi^n\|_M^2 + C\|c_{f0}\|_M^2.
\end{aligned}\tag{56}$$

Combining Eq. (53) with Eq. (56) and using Gronwall's inequality lead to

$$\begin{aligned}
&\sum_{n=1}^{m}\Delta t\|d_t\Psi^n\|_M^2 + \|\Psi^m\|_M^2 + \|\boldsymbol{Q}^m\|_{TM}^2 + \sum_{n=1}^{m}\Delta t\|\boldsymbol{Q}^n\|_{TM}^2\\
&\quad\leq C\sum_{n=1}^{m}\Delta t\|f_I^n c_I^n\|_M^2 + C\sum_{n=1}^{m}\Delta t\|d_t Z^n\|_M^2\\
&\qquad + C\|\boldsymbol{q}_0\|_{TM}^2 + C\|c_{f0}\|_M^2.
\end{aligned}\tag{57}$$

Taking notice of Eq. (42), we have

$$\begin{aligned}
&\sum_{n=1}^{m}\Delta t\|d_t\Psi^n\|_M^2 + \|\Psi^m\|_M^2 + \|\boldsymbol{Q}^m\|_{TM}^2 + \sum_{n=1}^{m}\Delta t\|\boldsymbol{Q}^n\|_{TM}^2\\
&\quad\leq C\sum_{n=1}^{m}\Delta t\|f_I^n c_I^n\|_M^2 + C\sum_{n=1}^{m}\Delta t\|f^n\|_M^2\\
&\qquad + C\left(\|\boldsymbol{q}_0\|_{TM}^2 + \|\boldsymbol{u}_0\|_{TM}^2 + \|c_{f0}\|_M^2 + r_\phi^{*2}\right).
\end{aligned}\tag{58}$$

Then the proof ends. □

5 Error Analysis for the Discrete Scheme

In this section, to give the error estimates, we consider the following elliptic projections first.

Let $\underline{Z}^n \in S_h$, $\underline{\mathbf{W}}^n \in \mathbf{V}_h^0$ be defined by

$$(\nabla \cdot \underline{\mathbf{W}}^n, w) = (\nabla \cdot \mathbf{u}^n, w), \quad \forall w \in S_h, \tag{59}$$

$$\left(\frac{\mu}{K(\phi^n)}\underline{\mathbf{W}}^n, \boldsymbol{v}\right)_{TM} = (\underline{Z}^n, \nabla \cdot \boldsymbol{v}), \quad \forall \boldsymbol{v} \in \mathbf{V}_h^0. \tag{60}$$

And $\underline{\Psi}^n \in S_h$, $\underline{\mathbf{Q}}^n \in \mathbf{V}_h^0$ be defined by

$$(\nabla \cdot \underline{\mathbf{Q}}^n, w) = (\nabla \cdot \mathbf{q}^n, w), \quad \forall w \in S_h, \tag{61}$$

$$((\phi^n \mathbf{D}^n)^{-1}\underline{\mathbf{Q}}^n, \boldsymbol{v})_{TM} = (\underline{\Psi}^n, \nabla \cdot \boldsymbol{v}), \quad \forall \boldsymbol{v} \in \mathbf{V}_h^0. \tag{62}$$

Set

$$\begin{cases} E_{\mathbf{u}}^A = \mathbf{W} - \underline{\mathbf{W}}, \quad E_{\mathbf{u}}^B = \underline{\mathbf{W}} - \mathbf{u}, \\ E_p^A = Z - \underline{Z}, \quad E_p^B = \underline{Z} - p, \\ E_{\mathbf{q}}^A = \mathbf{Q} - \underline{\mathbf{Q}}, \quad E_{\mathbf{q}}^B = \underline{\mathbf{Q}} - \mathbf{q}, \\ E_{c_f}^A = \Psi - \underline{\Psi}, \quad E_{c_f}^B = \underline{\Psi} - c_f, \\ E_\phi = \Theta - \phi. \end{cases} \tag{63}$$

Assume $(H1)$–$(H5)$ hold, it's shown by Dawson et al. in [21] that preliminary functions defined by Eqs. (59)–(62) exist and are unique. Besides, the error estimates are illustrated in Lemma 5.

Lemma 5 *Assume $(H1)$–$(H5)$ hold, then there exists a positive constant C independent of h and Δt such that*

$$\|d_t E_p^{B,m}\|_M + \|E_p^{B,m}\|_M + \|E_{\boldsymbol{u}}^{B,m}\|_{TM} \le C\left(\Delta t + h^2\right), \quad m \le N. \tag{64}$$

$$\|d_t E_{c_f}^{B,m}\|_M + \|E_{c_f}^{B,m}\|_M + \|E_{\boldsymbol{q}}^{B,m}\|_{TM} \le C\left(\Delta t + h^2\right), \quad m \le N. \tag{65}$$

Lemma 6 *The approximate errors of discrete porosity satisfy*

$$\|E_\phi^m\|_M^2 \le C\sum_{n=1}^m \Delta t\left(\|E_\phi^n\|_M^2 + \|E_{c_f}^{A,n-1}\|_M^2\right) + C\left(\Delta t^2 + h^4\right), \tag{66}$$

$$\sum_{n=1}^m \Delta t\|d_t E_\phi^n\|_M^2 \le C\sum_{n=1}^m \Delta t\left(\|E_\phi^n\|_M^2 + \|E_{c_f}^{A,n-1}\|_M^2\right) + C\left(\Delta t^2 + h^4\right), \quad m \le N, \tag{67}$$

where the positive constant C is independent of h and Δt.

Proof Subtracting Eq. (21) from Eq. (26), we can obtain

$$
\begin{aligned}
d_t E^n_{\phi,i,j} &= \frac{r^n_{\phi,i,j}\left(1-\Theta^n_{i,j}\right)}{1-\phi_{0,i,j}}\overline{\Psi}^{n-1}_{i,j} - \frac{r^n_{\phi,i,j}\left(1-\phi^n_{i,j}\right)}{1-\phi_{0,i,j}}c^n_{f,i,j} + \frac{\partial \phi^n_{i,j}}{\partial t} - d_t\phi^n_{i,j} \\
&= \frac{r^n_{\phi,i,j}\left(1-\Theta^n_{i,j}\right)}{1-\phi_{0,i,j}}\left(\overline{\Psi}^{n-1}_{i,j} - c^{n-1}_{f,i,j}\right) + \frac{r^n_{\phi,i,j}\left(1-\Theta^n_{i,j}\right)}{1-\phi_{0,i,j}}\left(c^{n-1}_{f,i,j} - c^n_{f,i,j}\right) \\
&\quad - \frac{r^n_{\phi,i,j}c^n_{f,i,j}}{1-\phi_{0,i,j}}E^n_{\phi,i,j} + R^n_1,
\end{aligned} \tag{68}
$$

where $R^n_1 = \dfrac{\partial \phi^n_{i,j}}{\partial t} - d_t\phi^n_{i,j}$.
Multiplying Eq. (68) by $E^n_{\phi,i,j}h^x_i h^y_j$ and making summation on i, j for $1 \leq i \leq N_x,\ 1 \leq j \leq N_y$, we have that

$$
\begin{aligned}
&(d_t E^n_\phi, E^n_\phi)_M \\
&= \left(\frac{r^n_\phi(1-\Theta^n)}{1-\phi_0}\left(\overline{\Psi}^{n-1} - c^{n-1}_f\right), E^n_\phi\right)_M + \left(\frac{r^n_\phi(1-\Theta^n)}{1-\phi_0}\left(c^{n-1}_f - c^n_f\right), E^n_\phi\right)_M \\
&\quad - \left(\frac{r^n_\phi c^n_f}{1-\phi_0}E^n_\phi, E^n_\phi\right)_M + \left(R^n_1, E^n_\phi\right)_M.
\end{aligned} \tag{69}
$$

The term in the left side of Eq. (69) can be transformed into

$$
(d_t E^n_\phi, E^n_\phi)_M = \frac{\|E^n_\phi\|^2_M - \|E^{n-1}_\phi\|^2_M}{2\Delta t} + \frac{\Delta t}{2}\|d_t E^n_\phi\|^2_M. \tag{70}
$$

Taking notice of Lemma 5, the first term in the right side of Eq. (69) can be estimated by

$$
\begin{aligned}
\left(\frac{r^n_\phi(1-\Theta^n)}{1-\phi_0}\left(\overline{\Psi}^{n-1} - c^{n-1}_f\right), E^n_\phi\right)_M &\leq \frac{r^*_\phi}{2}\left(\|E^{A,n-1}_{c_f} + E^{B,n-1}_{c_f}\|^2_M + \|E^n_\phi\|^2_M\right) \\
&\leq \frac{r^*_\phi}{2}\left(\|E^{A,n-1}_{c_f}\|^2_M + \|E^n_\phi\|^2_M\right) + C\left(\Delta t^2 + h^4\right),
\end{aligned} \tag{71}
$$

where we used the fact that $|\overline{\Psi}^{n-1} - c^{n-1}_f| \leq |\Psi^{n-1} - c^{n-1}_f|$.
Noting the smoothness assumption $(H1)$, the second term in the right side of Eq. (69) can be bounded by

$$
\left(\frac{r^n_\phi(1-\Theta^n)}{1-\phi_0}\left(c^{n-1}_f - c^n_f\right), E^n_\phi\right)_M \leq \frac{r^*_\phi}{2}\|E^n_\phi\|^2_M + C\Delta t^2. \tag{72}
$$

Combing Eq. (69) with Eqs. (70)–(72), multiplying by $2\Delta t$, and summing for n from 1 to m, $m \leq N$, we have

$$
\|E^m_\phi\|^2_M \leq \|E^0_\phi\|^2_M + C\Delta t\sum_{n=1}^{m}\|E^{A,n-1}_{c_f}\|^2_M + C\Delta t\sum_{n=1}^{m}\|E^n_\phi\|^2_M + C\left(\Delta t^2 + h^4\right). \tag{73}
$$

Recalling the initial condition on T^0 gives Eq. (66).

On the other hand, multiplying Eq. (68) by $d_t E^n_{\phi,i,j} h^x_i h^y_j$ and making summation on i, j for $1 \leq i \leq N_x,\ 1 \leq j \leq N_y$, we have that

$$\|d_t E^n_\phi\|^2_M = \left(\frac{r^n_\phi(1-\Theta^n)}{1-\phi_0}\left(\overline{\Psi}^{n-1} - c^{n-1}_f\right), d_t E^n_\phi\right)_M + \left(\frac{r^n_\phi(1-\Theta^n)}{1-\phi_0}\left(c^{n-1}_f - c^n_f\right), d_t E^n_\phi\right)_M - \left(\frac{r^n_\phi c^n_f}{1-\phi_0} E^n_\phi, d_t E^n_\phi\right)_M + \left(R^n_1, d_t E^n_\phi\right)_M. \tag{74}$$

Similarly we can obtain that

$$\sum_{n=1}^m \Delta t \|d_t E^n_\phi\|^2_M \leq C \sum_{n=1}^m \Delta t \|E^n_\phi\|^2_M + C \sum_{n=1}^m \Delta t \|E^{A,n-1}_{c_f}\|^2_M + C\left(\Delta t^2 + h^4\right).$$

Then the proof ends. □

Lemma 7 *The approximate errors of discrete pressure and velocity satisfy*

$$\gamma \sum_{n=1}^m \Delta t \|d_t E^{A,n}_p\|^2_M + \|\frac{\mu}{K(\Pi_h \Theta^m)} E^{A,m}_{\boldsymbol{u}}\|^2_{TM} \leq C \sum_{n=1}^m \Delta t \left(\|E^n_\phi\|^2_M + \|d_t E^n_\phi\|^2_M\right) + C \sum_{n=1}^m \Delta t \|E^{A,n}_{\boldsymbol{u}}\|^2_{TM} + C\left(\Delta t^2 + h^4\right), \quad m \leq N,$$

where the positive constant C is independent of h and $\triangle t$.

Proof Subtracting Eq. (59) from Eq. (22), we have that

$$\left(\gamma d_t Z^n + d_t \Theta^n, w\right) + \left(\nabla \cdot E^{A,n}_{\mathbf{u}}, w\right) = \left(\gamma \frac{\partial p^n}{\partial t} + \frac{\partial \phi^n}{\partial t}, w\right). \tag{75}$$

We can get the following equation by subtracting Eq. (60) from Eq. (23).

$$\left(\frac{\mu}{K(\Pi_h \Theta^n)} \boldsymbol{W}^n, \boldsymbol{v}\right)_{TM} - \left(\frac{\mu}{K(\phi^n)} \underline{\mathbf{W}}^n, \boldsymbol{v}\right)_{TM} = \left(E^{A,n}_p, \nabla \cdot \mathbf{v}\right), \quad \forall \boldsymbol{v} \in \mathbf{V}^0_h. \tag{76}$$

By Eq. (76), we have that

$$\left(d_t\left(\frac{\mu}{K(\Pi_h \Theta^n)} \boldsymbol{W}^n - \frac{\mu}{K(\phi^n)} \underline{\mathbf{W}}^n\right), \boldsymbol{v}\right)_{TM} = \left(d_t E^{A,n}_p, \nabla \cdot \boldsymbol{v}\right), \quad \forall \boldsymbol{v} \in \mathbf{V}^0_h. \tag{77}$$

Setting $w = d_t E^{A,n}_p$ and $\boldsymbol{v} = E^{A,n}_{\mathbf{u}}$ in Eqs. (75) and (77) respectively, we have

$$\gamma \|d_t E^{A,n}_p\|^2_M + \left(\nabla \cdot E^{A,n}_{\mathbf{u}}, d_t E^{A,n}_p\right) = \gamma\left(\frac{\partial p^n}{\partial t} - d_t p^n, d_t E^{A,n}_p\right) - \gamma\left(d_t E^{B,n}_p, d_t E^{A,n}_p\right) - \left(d_t E^n_\phi, d_t E^{A,n}_p\right) + \left(\frac{\partial \phi^n}{\partial t} - d_t \phi^n, d_t E^{A,n}_p\right), \tag{78}$$

and

$$\left(d_t\left(\frac{\mu}{K(\Pi_h \Theta^n)} \boldsymbol{W}^n - \frac{\mu}{K(\phi^n)} \underline{\mathbf{W}}^n\right), E^{A,n}_{\mathbf{u}}\right)_{TM} = \left(d_t E^{A,n}_p, \nabla \cdot E^{A,n}_{\mathbf{u}}\right). \tag{79}$$

By Cauchy–Schwarz inequality, the first term in the right hand side of Eq. (78) can be estimated by

$$\gamma\left(\frac{\partial p^n}{\partial t}-d_t p^n, d_t E_p^{A,n}\right) \le C\|p\|^2_{W_2^\infty(t^{n-1},t^n;L^\infty(\Omega))}\Delta t^2+\frac{\gamma}{8}\|d_t E_p^{A,n}\|_M^2. \tag{80}$$

The second term in the right hand side of Eq. (78) can be estimated by

$$\gamma\left(d_t E_p^{B,n}, d_t E_p^{A,n}\right) \le C\|d_t E_p^{B,n}\|_M^2+\frac{\gamma}{8}\|d_t E_p^{A,n}\|_M^2. \tag{81}$$

Easily we have

$$\left(d_t E_\phi^n, d_t E_p^{A,n}\right) \le C\|d_t E_\phi^n\|_M^2+\frac{\gamma}{8}\|d_t E_p^{A,n}\|_M^2, \tag{82}$$

and

$$\left(\frac{\partial \phi^n}{\partial t}-d_t\phi^n, d_t E_p^{A,n}\right) \le C\|\phi\|^2_{W_2^\infty(t^{n-1},t^n;L^\infty(\Omega))}\Delta t^2+\frac{\gamma}{8}\|d_t E_p^{A,n}\|_M^2. \tag{83}$$

The term in the left hand side of Eq. (79) can be transformed into

$$\begin{aligned}&\left(d_t\left(\frac{\mu}{K(\Pi_h\Theta^n)}\boldsymbol{W}^n-\frac{\mu}{K(\phi^n)}\underline{\mathbf{W}}^n\right), E_{\mathbf{u}}^{A,n}\right)_{TM}\\ &=\left(d_t\left(\frac{\mu}{K(\Pi_h\Theta^n)}E_{\mathbf{u}}^{A,n}\right), E_{\mathbf{u}}^{A,n}\right)_{TM}\\ &\quad+\left(d_t\left(\left(\frac{\mu}{K(\Pi_h\Theta^n)}-\frac{\mu}{K(\phi^n)}\right)\underline{\mathbf{W}}^n\right), E_{\mathbf{u}}^{A,n}\right)_{TM}.\end{aligned} \tag{84}$$

The first term in the right hand side of Eq. (84) can be estimated by

$$\begin{aligned}&\left(d_t\left(\frac{\mu}{K(\Pi_h\Theta^n)}E_{\mathbf{u}}^{A,n}\right), E_{\mathbf{u}}^{A,n}\right)_{TM}=\frac{1}{2}d_t\|\frac{\mu}{K(\Pi_h\Theta^n)}E_{\mathbf{u}}^{A,n}\|_{TM}^2\\ &+\frac{\Delta t}{2}\frac{\mu}{K(\Pi_h\Theta^{n-1})}\|d_t E_{\mathbf{u}}^{A,n}\|_{TM}^2\\ &+\frac{1}{2}\left(d_t(\frac{\mu}{K(\Pi_h\Theta^n)})E_{\mathbf{u}}^{A,n}, E_{\mathbf{u}}^{A,n}\right)_{TM}.\end{aligned} \tag{85}$$

The second term in the right hand side of Eq. (84) can be bounded by

$$\begin{aligned}&\left(d_t\left((\frac{\mu}{K(\Pi_h\Theta^n)}-\frac{\mu}{K(\phi^n)})\underline{\mathbf{W}}^n\right), E_{\mathbf{u}}^{A,n}\right)_{TM}\\ &=\left(d_t\left(\frac{\mu}{K(\Pi_h\Theta^n)}-\frac{\mu}{K(\phi^n)}\right)\underline{\mathbf{W}}^n, E_{\mathbf{u}}^{A,n}\right)_{TM}\\ &\quad+\left((\frac{\mu}{K(\Pi_h\Theta^n)}-\frac{\mu}{K(\phi^n)})d_t\underline{\mathbf{W}}^n, E_{\mathbf{u}}^{A,n}\right)_{TM}\end{aligned} \tag{86}$$

Then, we prove the boundedness of $\|\underline{\mathbf{W}}^n\|_\infty$, which is necessary in the following estimates. By the triangle inequality,

$$\|\underline{\mathbf{W}}^n\|_\infty \le \|\underline{\mathbf{W}}^n-\hat{\boldsymbol{u}}^n\|_\infty+\|\hat{\boldsymbol{u}}^n-\boldsymbol{u}^n\|_\infty+\|\boldsymbol{u}^n\|_\infty.$$

Taking notice of the inverse assumption and the triangle inequality, we have

$$\begin{aligned}\|\underline{\mathbf{W}}^n-\hat{\boldsymbol{u}}^n\|_\infty &\le Ch^{-1}\|\underline{\mathbf{W}}^n-\hat{\boldsymbol{u}}^n\|_{TM}\\ &\le Ch^{-1}\left(\|\underline{\mathbf{W}}^n-\boldsymbol{u}^n\|_{TM}+\|\boldsymbol{u}^n-\hat{\boldsymbol{u}}^n\|_{TM}\right).\end{aligned}$$

Then using Eqs. (14), (15) and Lemma 5, we obtain

$$\begin{aligned}\|\underline{\mathbf{W}}^n\|_\infty &\leq Ch^{-1}\left(\|\underline{\mathbf{W}}^n - \boldsymbol{u}^n\|_{TM} + \|\boldsymbol{u}^n - \hat{\boldsymbol{u}}^n\|_{TM}\right) + \|\hat{\boldsymbol{u}}^n - \boldsymbol{u}^n\|_\infty + \|\boldsymbol{u}^n\|_\infty \\ &\leq Ch^{-1}(h^2 + \Delta t) + \|\boldsymbol{u}^n\|_\infty \leq C_1, \end{aligned} \tag{87}$$

where $h,\ \triangle t$ are selected such that $h^{-1}\triangle t$ is sufficiently small and similar to the derivation of Eq. (87), we can obtain that

$$\|d_t\underline{\mathbf{W}}^n\|_\infty \leq C_2. \tag{88}$$

Noting the definition of Π_h, the first term in the right hand side of Eq. (86) can be bounded by

$$\begin{aligned}&\left(d_t\left(\frac{\mu}{K(\Pi_h\Theta^n)} - \frac{\mu}{K(\phi^n)}\right)\underline{\mathbf{W}}^n, E_{\mathbf{u}}^{A,n}\right)_{TM} \\ &= \left(d_t\left(\frac{\mu}{K(\Pi_h\Theta^n)} - \frac{\mu}{K(\Pi_h\phi^n)}\right)\underline{\mathbf{W}}^n, E_{\mathbf{u}}^{A,n}\right)_{TM} \\ &\quad + \left(d_t\left(\frac{\mu}{K(\Pi_h\phi^n)} - \frac{\mu}{K(\phi^n)}\right)\underline{\mathbf{W}}^n, E_{\mathbf{u}}^{A,n}\right)_{TM} \\ &\leq C\left\|\frac{\partial^3(\mu K^{-1})}{\partial\phi\partial t^2}\right\|_{L^\infty(t^{n-1},t^n;L^\infty(\mathbb{R}))}\left(\|E_\phi^n\|_M^2 + \|\Pi_h\phi^n - \phi^n\|_M^2\right) + C\|E_{\mathbf{u}}^{A,n}\|_{TM}^2 \\ &\quad + C\left\|\frac{\partial(\mu K^{-1})}{\partial\phi}\right\|_{L^\infty(\mathbb{R})}\left(\|d_tE_\phi^n\|_M^2 + \|d_t(\Pi_h\phi^n - \phi^n)\|_M^2\right). \end{aligned} \tag{89}$$

By the boundedness of $\|d_t\underline{\mathbf{W}}^n\|_\infty$, the second term in the right hand side of Eq. (86) can be bounded by

$$\begin{aligned}&\left(\left(\frac{\mu}{K(\Pi_h\Theta^n)} - \frac{\mu}{K(\phi^n)}\right)d_t\underline{\mathbf{W}}^n, E_{\mathbf{u}}^{A,n}\right)_{TM} \\ &\quad \leq C\left\|\frac{\partial(\mu K^{-1})}{\partial\phi}\right\|_{L^\infty(\mathbb{R})}\left(\|E_\phi^n\|_M^2 + \|\Pi_h\phi^n - \phi^n\|_M^2\right) + C\|E_{\mathbf{u}}^{A,n}\|_{TM}^2. \end{aligned} \tag{90}$$

Combining the above equations and noting Lemma 5, we obtain

$$\begin{aligned}&\frac{\gamma}{2}\|d_tE_p^{A,n}\|_M^2 + \frac{1}{2}d_t\|\frac{\mu}{K(\Pi_h\Theta^n)}E_{\mathbf{u}}^{A,n}\|_{TM}^2 \\ &\quad \leq C\left(\|E_\phi^n\|_M^2 + \|d_tE_\phi^n\|_M^2\right) + C\|E_{\mathbf{u}}^{A,n}\|_{TM}^2 + C\left(\Delta t^2 + h^4\right). \end{aligned} \tag{91}$$

Multiplying by $2\Delta t$, and summing for n from 1 to m, $m \leq N$, we have

$$\begin{aligned}&\gamma\sum_{n=1}^m \Delta t\|d_tE_p^{A,n}\|_M^2 + \left\|\frac{\mu}{K(\Pi_h\Theta^m)}E_{\mathbf{u}}^{A,m}\right\|_{TM}^2 \\ &\quad \leq C\sum_{n=1}^m \Delta t\left(\|E_\phi^n\|_M^2 + \|d_tE_\phi^n\|_M^2\right) + C\sum_{n=1}^m \Delta t\|E_{\mathbf{u}}^{A,n}\|_{TM}^2 \\ &\qquad + C\left(\Delta t^2 + h^4\right). \end{aligned} \tag{92}$$

Then the proof ends. □

Lemma 8 *The approximate errors of discrete concentration and flux variable satisfy*

$$\phi_{0*}\sum_{n=1}^{m}\Delta t\|d_t E_{c_f}^{A,n}\|_M^2+\|E_{c_f}^{A,m}\|_M^2+\|(\Pi_h\Theta^m\boldsymbol{D})^{-1}E_{\boldsymbol{q}}^{A,m}\|_{TM}^2+C\sum_{n=1}^{m}\Delta t\|E_{\boldsymbol{q}}^{A,n}\|_{TM}^2$$
$$\leq C\sum_{n=1}^{m}\Delta t\left(\|E_\phi^n\|_M^2+\|d_t E_\phi^n\|_M^2\right)+C\sum_{n=1}^{m}\Delta t\|d_t E_p^{A,n}\|_M^2$$
$$+C\sum_{n=1}^{m}\Delta t\left(\|E_{\boldsymbol{q}}^{A,n}\|_{TM}^2+\|E_{\boldsymbol{u}}^{A,n}\|_{TM}^2\right)$$
$$+C\left(\Delta t^2+h^4\right), \tag{93}$$

where the positive constant C is independent of h and $\triangle t$.

Proof Subtracting Eq. (61) from Eq. (24), we have that

$$\begin{aligned}&(\Theta^n d_t\Psi^n,w)-(\gamma\overline{\Psi}^{n-1}d_t Z^n,w)-\left((\Theta^n\mathbf{D})^{-1}\Pi_h\mathbf{W}^n\cdot\Pi_h\mathbf{Q}^n,w\right)\\&\quad+\left(\nabla\cdot E_{\mathbf{q}}^{A,n},w\right)+\left(f_I^n\Psi^n,w\right)+\frac{k_ck_s}{k_c+k_s}\left(a_v(\Theta^n)\Psi^n,w\right)\\&=\phi^n\frac{\partial c_f^n}{\partial t}-\gamma c_f^n\frac{\partial p^n}{\partial t}-\left((\phi^n\mathbf{D})^{-1}\mathbf{u}^n\cdot\mathbf{q}^n+f_I^nc_f^n,w\right)\\&\quad+\frac{k_ck_s}{k_c+k_s}\left(a_v(\phi^n)c_f^n,w\right),\quad\forall w\in S_h.\end{aligned} \tag{94}$$

And subtracting Eq. (62) from Eq. (25), we can obtain

$$\left((\Pi_h\Theta^n\mathbf{D})^{-1}\boldsymbol{Q}^n,\boldsymbol{v}\right)_{TM}-\left((\phi^n\mathbf{D})^{-1}\underline{\mathbf{Q}}^n,\boldsymbol{v}\right)_{TM}=\left(E_{c_f}^{A,n},\nabla\cdot\boldsymbol{v}\right),\quad\forall\boldsymbol{v}\in\mathbf{V}_h^0. \tag{95}$$

By Eq. (95), we have that

$$\left(d_t\left((\Pi_h\Theta^n\mathbf{D})^{-1}\boldsymbol{Q}^n-(\phi^n\mathbf{D})^{-1}\underline{\mathbf{Q}}^n\right),\boldsymbol{v}\right)_{TM}=\left(d_tE_{c_f}^{A,n},\nabla\cdot\boldsymbol{v}\right),\quad\forall\boldsymbol{v}\in\mathbf{V}_h^0, \tag{96}$$

Set $w=d_tE_{c_f}^{A,n}$ and $\boldsymbol{v}=E_{\mathbf{q}}^{A,n}$ in Eqs. (94) and (96) respectively, we have

$$\begin{aligned}&\left(\Theta^n d_tE_{c_f}^{A,n},d_tE_{c_f}^{A,n}\right)+\left(\nabla\cdot E_{\mathbf{q}}^{A,n},d_tE_{c_f}^{A,n}\right)\\&=\left(\phi^n\frac{\partial c_f^n}{\partial t}-\Theta^n d_t\underline{\Psi}^n,d_tE_{c_f}^{A,n}\right)-\left(\gamma c_f^n\frac{\partial p^n}{\partial t}-\gamma\overline{\Psi}^{n-1}d_tZ^n,d_tE_{c_f}^{A,n}\right)\\&\quad+\left((\Theta^n\mathbf{D})^{-1}\Pi_h\mathbf{W}^n\cdot\Pi_h\mathbf{Q}^n-(\phi^n\mathbf{D})^{-1}\mathbf{u}^n\cdot\mathbf{q}^n,d_tE_{c_f}^{A,n}\right)\\&\quad-\frac{k_ck_s}{k_c+k_s}\left(a_v(\Theta^n)\Psi^n-a_v(\phi^n)c_f^n,d_tE_{c_f}^{A,n}\right)\\&\quad-\left(f_I^n(\Psi^n-c_f^n),d_tE_{c_f}^{A,n}\right),\end{aligned} \tag{97}$$

and

$$\left(d_t\left((\Pi_h\Theta^n\mathbf{D})^{-1}\boldsymbol{Q}^n-(\phi^n\mathbf{D})^{-1}\underline{\mathbf{Q}}^n\right),E_{\mathbf{q}}^{A,n}\right)_{TM}=\left(d_tE_{c_f}^{A,n},\nabla\cdot E_{\mathbf{q}}^{A,n}\right). \tag{98}$$

By Cauchy–Schwarz inequality, the first term in the right hand side of Eq. (97) can be estimated by

$$\begin{aligned}
&\left(\phi^n \frac{\partial c_f^n}{\partial t} - \Theta^n d_t \underline{\Psi}^n, d_t E_{c_f}^{A,n}\right) \\
&= \left((\phi^n - \Theta^n)\frac{\partial c_f^n}{\partial t}, d_t E_{c_f}^{A,n}\right) + \left(\Theta^n \left(\frac{\partial c_f^n}{\partial t} - d_t c_f^n\right), d_t E_{c_f}^{A,n}\right) \\
&\quad - \left(\Theta^n d_t E_{c_f}^{B,n}, d_t E_{c_f}^{A,n}\right) \\
&\le C\|c_f\|^2_{W_1^\infty(J;L^\infty(\Omega))}\|E_\phi^n\|_M^2 + C\|\Theta\|^2_{L^\infty(J;L^\infty(\Omega))}\|c_f\|^2_{W_2^\infty(J;L^\infty(\Omega))}\Delta t^2 \\
&\quad + C\|\Theta\|^2_{L^\infty(J;L^\infty(\Omega))}\|d_t E_{c_f}^{B,n}\|_M^2 + \frac{\phi_{0*}}{14}\|d_t E_{c_f}^{A,n}\|_M^2.
\end{aligned} \tag{99}$$

The second term in the right hand side of Eq. (97) can be estimated by

$$\begin{aligned}
&\gamma\left(c_f^n \frac{\partial p^n}{\partial t} - \overline{\Psi}^{n-1} d_t Z^n, d_t E_{c_f}^{A,n}\right) \\
&= \gamma\left(\left(c_f^n - \overline{\Psi}^{n-1}\right)\frac{\partial p^n}{\partial t}, d_t E_{c_f}^{A,n}\right) + \gamma\left(\overline{\Psi}^{n-1}\left(\frac{\partial p^n}{\partial t} - d_t p^n\right), d_t E_{c_f}^{A,n}\right) \\
&\quad - \gamma\left(\overline{\Psi}^{n-1}\left(d_t E_p^{A,n} + d_t E_p^{B,n}\right), d_t E_{c_f}^{A,n}\right) \\
&\le C\|p\|^2_{W_1^\infty(J;L^\infty(\Omega))}\left(\|E_{c_f}^{A,n}\|_M^2 + \|E_{c_f}^{B,n}\|_M^2 + \|c_f\|^2_{W_1^\infty(J;L^\infty(\Omega))}\Delta t^2\right) \\
&\quad + C\|\overline{\Psi}\|^2_{L^\infty(J;L^\infty(\Omega))}\|p\|^2_{W_2^\infty(J;L^\infty(\Omega))}\Delta t^2 + \frac{\phi_{0*}}{14}\|d_t E_{c_f}^{A,n}\|_M^2 \\
&\quad + C\|\overline{\Psi}\|^2_{L^\infty(J;L^\infty(\Omega))}\left(\|d_t E_p^{A,n}\|_M^2 + \|d_t E_p^{B,n}\|_M^2\right).
\end{aligned} \tag{100}$$

The third term in the right hand side of Eq. (97) can be estimated by

$$\begin{aligned}
&\left((\Theta^n \mathbf{D})^{-1}\Pi_h \mathbf{W}^n \cdot \Pi_h \mathbf{Q}^n - (\phi^n \mathbf{D})^{-1}\mathbf{u}^n \cdot \mathbf{q}^n, d_t E_{c_f}^{A,n}\right) \\
&= \left((\Theta^n \mathbf{D})^{-1}\Pi_h \mathbf{W}^n \cdot (\Pi_h \mathbf{Q}^n - \mathbf{q}^n), d_t E_{c_f}^{A,n}\right) \\
&\quad + \left((\Theta^n \mathbf{D})^{-1}(\Pi_h \mathbf{W}^n - \mathbf{u}^n) \cdot \mathbf{q}^n, d_t E_{c_f}^{A,n}\right) \\
&\quad + \left((\Theta^{-n} - \phi^{-n})\mathbf{D}^{-1}\mathbf{u}^n \cdot \mathbf{q}^n, d_t E_{c_f}^{A,n}\right)
\end{aligned} \tag{101}$$

The first term in the right hand side of Eq. (101) can be estimated by

$$\begin{aligned}
&\left((\Theta^n \mathbf{D})^{-1}\Pi_h \mathbf{W}^n \cdot (\Pi_h \mathbf{Q}^n - \mathbf{q}^n), d_t E_{c_f}^{A,n}\right) \\
&\le C\|(\Theta^n \mathbf{D})^{-1}\Pi_h \mathbf{W}^n\|^2_{L^\infty(\Omega)}\left(\|\Pi_h \mathbf{Q}^n - \Pi_h \mathbf{q}^n\|_M^2 + \|\Pi_h \mathbf{q}^n - \mathbf{q}^n\|_M^2\right) + \frac{\phi_{0*}}{14}\|d_t E_{c_f}^{A,n}\|_M^2 \\
&\le C\left(\|E_{\mathbf{q}}^{A,n}\|_{TM}^2 + \|E_{\mathbf{q}}^{B,n}\|_{TM}^2\right) + \frac{\phi_{0*}}{14}\|d_t E_{c_f}^{A,n}\|_M^2 + Ch^4.
\end{aligned} \tag{102}$$

The second term in the right hand side of Eq. (101) can be estimated by

$$\begin{aligned}&\left((\Theta^n\mathbf{D})^{-1}(\Pi_h\mathbf{W}^n-\mathbf{u}^n)\cdot\mathbf{q}^n, d_tE_{c_f}^{A,n}\right)\\ &\quad\le C\|(\Theta^n\mathbf{D})^{-1}\mathbf{q}^n\|_{L^\infty(\Omega)}^2\left(\|\Pi_h\mathbf{W}^n-\Pi_h\mathbf{u}^n\|_M^2+\|\Pi_h\mathbf{u}^n-\mathbf{u}^n\|_M^2\right)+\frac{\phi_{0*}}{14}\|d_tE_{c_f}^{A,n}\|_M^2\\ &\quad\le C(\|E_{\mathbf{u}}^{A,n}\|_{TM}^2+\|E_{\mathbf{u}}^{B,n}\|_{TM}^2)+\frac{\phi_{0*}}{14}\|d_tE_{c_f}^{A,n}\|_M^2+Ch^4. \end{aligned} \tag{103}$$

The last term in the right hand side of Eq. (101) can be estimated by

$$\left((\Theta^{-n}-\phi^{-n})\mathbf{D}^{-1}\mathbf{u}^n\cdot\mathbf{q}^n, d_tE_{c_f}^{A,n}\right)\le C\left\|\frac{\mathbf{u}^n\cdot\mathbf{q}^n}{\Theta^n\phi^n}\right\|_{L^\infty(\Omega)}\|E_\phi^n\|_M^2+\frac{\phi_{0*}}{14}\|d_tE_{c_f}^{A,n}\|_M^2. \tag{104}$$

Recalling that $0\le a_v(\Theta^n)\le a_0$ and $|a_v(\phi^n)-a_v(\Theta^n)|\le\frac{a_0}{1-\phi_0}|E_\phi|$, we can estimate the second to last term in the right hand side of Eq. (97) by

$$\begin{aligned}&\frac{k_ck_s}{k_c+k_s}\left(a_v(\phi^n)c_f^n-a_v(\Theta^n)\Psi^n, d_tE_{c_f}^{A,n}\right)\\ &\quad\le\frac{k_ck_s}{k_c+k_s}\left((a_v(\phi^n)-a_v(\Theta^n))c_f^n, d_tE_{c_f}^{A,n}\right)+\frac{k_ck_s}{k_c+k_s}\left(a_v(\Theta^n)(c_f^n-\Psi^n), d_tE_{c_f}^{A,n}\right)\\ &\quad\le C\|c_f^n\|_{L^\infty}^2\|E_\phi^n\|_M^2+\frac{\phi_{0*}}{14}\|d_tE_{c_f}^{A,n}\|_M^2+C\left(\Delta t^2+h^4\right). \end{aligned} \tag{105}$$

The last term in the right hand side of Eq. (97) can be estimated by

$$f_I^n(c_f^n-\Psi^n, d_tE_{c_f}^{A,n})\le C\|E_{c_f}^{A,n}\|_M^2+\frac{\phi_{0*}}{14}\|d_tE_{c_f}^{A,n}\|_M^2+C\left(\Delta t^2+h^4\right). \tag{106}$$

The term in the left hand side of Eq. (98) can be transformed into

$$\begin{aligned}&\left(d_t\left((\Pi_h\Theta^n\mathbf{D})^{-1}\boldsymbol{Q}^n-(\phi^n\mathbf{D})^{-1}\underline{\mathbf{Q}}^n\right), E_{\mathbf{q}}^{A,n}\right)_{TM}\\ &\quad=\left(d_t\left((\Pi_h\Theta^n\mathbf{D})^{-1}E_{\mathbf{q}}^{A,n}\right), E_{\mathbf{q}}^{A,n}\right)_{TM}\\ &\qquad+\left(d_t\left((\Pi_h\Theta^n\mathbf{D})^{-1}-(\phi^n\mathbf{D})^{-1})\underline{\mathbf{Q}}^n\right), E_{\mathbf{q}}^{A,n}\right)_{TM}. \end{aligned} \tag{107}$$

The first term in the right hand side of Eq. (107) can be estimated by

$$\begin{aligned}&\left(d_t\left((\Pi_h\Theta^n\mathbf{D})^{-1}E_{\mathbf{q}}^{A,n}\right), E_{\mathbf{q}}^{A,n}\right)_{TM}\\ &\quad=\frac{1}{2}d_t\|(\Pi_h\Theta^n\mathbf{D})^{-1}E_{\mathbf{q}}^{A,n}\|_{TM}^2+\frac{\Delta t}{2}(\Pi_h\Theta^{n-1}\mathbf{D})^{-1}\|d_tE_{\mathbf{q}}^{A,n}\|_{TM}^2\\ &\qquad+\frac{1}{2}\left(d_t((\Pi_h\Theta^n\mathbf{D})^{-1})E_{\mathbf{q}}^{A,n}, E_{\mathbf{q}}^{A,n}\right)_{TM}. \end{aligned} \tag{108}$$

The second term in the right hand side of Eq. (107) can be bounded by

$$\begin{aligned}&\left(d_t\left((\Pi_h\Theta^n\mathbf{D})^{-1}-(\phi^n\mathbf{D})^{-1})\underline{\mathbf{Q}}^n\right), E_{\mathbf{q}}^{A,n}\right)_{TM}\\ &\quad=\left(d_t\left((\Pi_h\Theta^n\mathbf{D})^{-1}-(\phi^n\mathbf{D})^{-1}\right)\underline{\mathbf{Q}}^n, E_{\mathbf{q}}^{A,n}\right)_{TM}\\ &\qquad+\left(((\Pi_h\Theta^n\mathbf{D})^{-1}-(\phi^n\mathbf{D})^{-1})d_t\underline{\mathbf{Q}}^n, E_{\mathbf{q}}^{A,n}\right)_{TM}. \end{aligned} \tag{109}$$

Similar to the derivations of Eqs. (87) and (89), the first term in the right hand side of Eq. (109) can be bounded by

$$\begin{aligned}&\left(d_t\left(\left(\Pi_h\Theta^n\mathbf{D}\right)^{-1}-\left(\phi^n\mathbf{D}\right)^{-1}\right)\underline{\mathbf{Q}}^n, E_{\mathbf{q}}^{A,n}\right)_{TM}\\&\quad\le C\|d_t(\Pi_h\Theta\mathbf{D}\phi)^{-1}\|_{L^\infty(t^{n-1},t^n;L^\infty(\mathbb{R}))}\left(\|E_\phi^n\|_M^2+\|\Pi_h\phi^n-\phi^n\|_M^2\right)+C\|E_{\mathbf{q}}^{A,n}\|_{TM}^2\\&\qquad+C\|(\Pi_h\Theta\mathbf{D}\phi)^{-1}\|_{L^\infty(t^{n-1},t^n;L^\infty(\mathbb{R}))}\left(\|d_tE_\phi^n\|_M^2+\|d_t(\Pi_h\phi^n-\phi^n)\|_M^2\right).\end{aligned}\tag{110}$$

Similar to the derivations of Eqs. (88) and (90), the second term in the right hand side of Eq. (109) can be bounded by

$$\begin{aligned}&\left(\left(\left(\Pi_h\Theta^n\mathbf{D}\right)^{-1}-\left(\phi^n\mathbf{D}\right)^{-1}\right)d_t\underline{\mathbf{Q}}^n, E_{\mathbf{q}}^{A,n}\right)_{TM}\\&\quad\le C\|(\Pi_h\Theta\mathbf{D}\phi)^{-1}\|_{L^\infty(t^{n-1},t^n;L^\infty(\mathbb{R}))}\left(\|E_\phi^n\|_M^2+\|\Pi_h\phi^n-\phi^n\|_M^2\right)+C\|E_{\mathbf{q}}^{A,n}\|_{TM}^2.\end{aligned}\tag{111}$$

Combining Eq. (97) with Eqs. (98)–(111), we can obtain

$$\begin{aligned}&\frac{\phi_{0*}}{2}\|d_tE_{c_f}^{A,n}\|_M^2+\frac{1}{2}d_t\|(\Pi_h\Theta^n\mathbf{D})^{-1}E_{\mathbf{q}}^{A,n}\|_{TM}^2\\&\quad\le C\left(\|E_\phi^n\|_M^2+\|d_tE_\phi^n\|_M^2\right)+C\left(\|E_{c_f}^{A,n}\|_M^2+\|d_tE_p^{A,n}\|_M^2\right)\\&\qquad+C\left(\|E_{\mathbf{q}}^{A,n}\|_{TM}^2+\|E_{\mathbf{u}}^{A,n}\|_{TM}^2\right)\\&\qquad+C\left(\Delta t^2+h^4\right).\end{aligned}\tag{112}$$

Multiplying by $2\Delta t$, and summing for n from 1 to m, $m\le N$, we have

$$\begin{aligned}&\phi_{0*}\sum_{n=1}^m\Delta t\|d_tE_{c_f}^{A,n}\|_M^2+\|(\Pi_h\Theta^m\mathbf{D})^{-1}E_{\mathbf{q}}^{A,m}\|_{TM}^2\\&\quad\le C\sum_{n=1}^m\Delta t\left(\|E_\phi^n\|_M^2+\|d_tE_\phi^n\|_M^2\right)+C\sum_{n=1}^m\Delta t\left(\|E_{c_f}^{A,n}\|_M^2+\|d_tE_p^{A,n}\|_M^2\right)\\&\qquad+C\sum_{n=1}^m\Delta t\left(\|E_{\mathbf{q}}^{A,n}\|_{TM}^2+\|E_{\mathbf{u}}^{A,n}\|_{TM}^2\right)\\&\qquad+C\left(\Delta t^2+h^4\right).\end{aligned}\tag{113}$$

Next we give the estimates for $\|E_{c_f}^{A,n}\|_M^2$. Taking $w=E_{c_f}^{A,n}$ and $\boldsymbol{v}=E_{\mathbf{q}}^{A,n}$ in Eqs. (94) and (95) respectively, we have

$$\begin{aligned}&\left(\Theta^nd_tE_{c_f}^{A,n},E_{c_f}^{A,n}\right)+\left(\nabla\cdot E_{\mathbf{q}}^{A,n},E_{c_f}^{A,n}\right)\\&\quad=\left(\phi^n\frac{\partial c_f^n}{\partial t}-\Theta^nd_t\underline{\Psi}^n,E_{c_f}^{A,n}\right)-\left(\gamma c_f^n\frac{\partial p^n}{\partial t}-\gamma\overline{\Psi}^{n-1}d_tZ^n,E_{c_f}^{A,n}\right)\\&\qquad+\left((\Theta^n\mathbf{D})^{-1}\Pi_h\mathbf{W}^n\cdot\Pi_h\mathbf{Q}^n-(\phi^n\mathbf{D})^{-1}\mathbf{u}^n\cdot\mathbf{q}^n,E_{c_f}^{A,n}\right)\\&\qquad-\frac{k_ck_s}{k_c+k_s}\left(a_v(\Theta^n)\Psi^n-a_v(\phi^n)c_f^n,E_{c_f}^{A,n}\right)\\&\qquad-\left(f_I^n\left(\Psi^n-c_f^n\right),E_{c_f}^{A,n}\right),\end{aligned}\tag{114}$$

and

$$\left((\Pi_h\Theta^n\mathbf{D})^{-1}\boldsymbol{Q}^n, E_{\mathbf{q}}^{A,n}\right)_{TM} - \left((\phi^n\mathbf{D})^{-1}\underline{\mathbf{Q}}^n, E_{\mathbf{q}}^{A,n}\right)_{TM} = \left(E_{c_f}^{A,n}, \nabla\cdot E_{\mathbf{q}}^{A,n}\right). \tag{115}$$

By the similar estimates with the above equations, we can easily obtain

$$\begin{aligned}
&\|E_{c_f}^{A,m}\|_M^2 + C\sum_{n=1}^m \Delta t\|(\Pi_h\Theta^n\mathbf{D})^{-1}E_{\mathbf{q}}^{A,n}\|_{TM}^2\\
&\le C\sum_{n=1}^m \Delta t\left(\|E_{c_f}^{A,n}\|_M^2 + \|d_t E_p^{A,n}\|_M^2 + \|E_\phi^n\|_M^2\right)\\
&\quad + C\sum_{n=1}^m \Delta t\|E_{\mathbf{u}}^{A,n}\|_{TM}^2 + C\left(\Delta t^2 + h^4\right).
\end{aligned} \tag{116}$$

Combining Eq. (113) with (116) and using Gronwall's inequality, we have

$$\begin{aligned}
&\phi_{0*}\sum_{n=1}^m \Delta t\|d_t E_{c_f}^{A,n}\|_M^2 + \|E_{c_f}^{A,m}\|_M^2 + \|(\Pi_h\Theta^m\mathbf{D})^{-1}E_{\mathbf{q}}^{A,m}\|_{TM}^2 + C\sum_{n=1}^m \Delta t\|E_{\mathbf{q}}^{A,n}\|_{TM}^2\\
&\le C\sum_{n=1}^m \Delta t\left(\|E_\phi^n\|_M^2 + \|d_t E_\phi^n\|_M^2\right) + C\sum_{n=1}^m \Delta t\|d_t E_p^{A,n}\|_M^2\\
&\quad + C\sum_{n=1}^m \Delta t\|E_{\mathbf{u}}^{A,n}\|_{TM}^2 + C\left(\Delta t^2 + h^4\right).
\end{aligned} \tag{117}$$

Then the proof ends. □

It remains to testify induction hypothesis (51). This proof is given through two steps.

Steps 1 (Definition of C^*): Using scheme (22)–(23) for $n = 0$ and Eq. (87), we can get the approximation $\boldsymbol{W}^1$ and the following property.

$$\begin{aligned}
\|\boldsymbol{W}^1\|_\infty &\le \|E_{\mathbf{u}}^{A,1}\|_\infty + \|\underline{\boldsymbol{W}}^1\|_\infty \le Ch^{-1}\|E_{\mathbf{u}}^{A,1}\|_{TM} + \|\underline{\boldsymbol{W}}^1\|_\infty\\
&\le C(h + h^{-1}\Delta t) + \|\underline{\boldsymbol{W}}^1\|_\infty \le C.
\end{aligned}$$

Thus define the positive constant C_* independent of h and Δt such that

$$C^* \ge \max\{\|\mathbf{W}^1\|_\infty, 2\|\underline{\mathbf{W}}^n\|_\infty\}.$$

Steps 2 (Induction): By the definition of C^*, it is trivial that hypothesis (51) holds true for $l = 1$. Supposing that $\|\Pi_h\mathbf{W}^{l-1}\|_\infty \le C^*$ holds true for an integer $l = 1, \dots, N-1$, by Lemmas 6–8 with $m = l$, we have that

$$\|E_{\mathbf{u}}^{A,l}\|_{TM} \le C(h^2 + \Delta t).$$

Next we prove that $\|\Pi_h\mathbf{W}^l\|_\infty \le C^*$ holds true. Since

$$\begin{aligned}
\|\mathbf{W}^l\|_\infty &\le \|E_{\mathbf{u}}^{A,l}\|_\infty + \|\underline{\boldsymbol{W}}^l\|_\infty \le Ch^{-1}\|E_{\mathbf{u}}^{A,l}\|_{TM} + \|\underline{\boldsymbol{W}}^l\|_\infty\\
&\le C_3(h + h^{-1}\Delta t) + \|\underline{\boldsymbol{W}}^l\|_\infty.
\end{aligned} \tag{118}$$

Let $\Delta t \le C_4h^2$ and a positive constant h_1 be small enough to satisfy

$$C_3(1 + C_4)h_1 \le \frac{C^*}{2}.$$

Then for $h \in (0, h_1]$, Eq. (118) can be estimated by

$$\begin{aligned}\|\mathbf{W}^l\|_\infty &\le C_3(h + h^{-1}\Delta t) + \|\underline{W}^l\|_\infty \\ &\le C_3(h_1 + C_4 h_1) + \frac{C^*}{2} \\ &\le C^*.\end{aligned}$$

It is obvious that

$$\|\Pi_h \mathbf{W}^l\|_\infty \le \|\mathbf{W}^l\|_\infty \le C^*,$$

then the proof ends.

Based on the above lemmas and using Gronwall's inequality, we have the main error estimates below.

Theorem 9 *Suppose* $(H1)$–$(H5)$ *hold then there exists a positive constant* C *independent of* h *and* $\triangle t$ *such that*

$$\begin{aligned}&\|(Z-p)^m\|_M + \|(\boldsymbol{W}-\boldsymbol{u})^m\|_{TM} + \|(\Psi - c_f)^m\|_M + \|(\boldsymbol{Q}-\boldsymbol{q})^m\|_{TM} \\ &\quad + \left(C\sum_{n=1}^{m}\Delta t\|(\boldsymbol{Q}-\boldsymbol{q})^n\|_{TM}^2\right)^{1/2} + \|(\Theta-\phi)^m\|_M^2 \\ &\le C(\Delta t + h^2), \quad m \le N.\end{aligned}$$

Remark 2 In our future work, we will consider the case that $\mathbf{D}$ is defined in Eq. (5). By using the similar technique in [10], it is supposed that the superconvergence rate $O(h^2 + \Delta t)$ is obtained for concentration of the acid and rate $O(h^{3/2} + \Delta t)$ for its flux in certain discrete norms. Besides, Examples 5 and 6 in the next section are presented to verify that the block-centered finite difference method is still effective for the case that $\mathbf{D}$ is not diagonal.

6 Numerical Examples

In this section, some numerical experiments using the block-centered finite difference method have been carried out.

We test Examples 1 and 2 to verify the convergence rates. The time step is refined as $\Delta t = 1/N_x^2 = 1/N_y^2$ to show the convergence and

$$\begin{cases}\mathbf{D} = 10^{-2}\,\mathbf{I}, \ K_0 = 1, \ \hat{T} = 0.5, \\ \alpha = k_c = k_s = \mu = f_I = 1, \\ a_0 = 0.5, \quad \rho_s = 10, \quad \gamma = 0.1,\end{cases}$$

where $\mathbf{I}$ is an identity matrix. In Example 1, the domain $\Omega = (0, 1) \times (0, 1)$ is uniformly divided by the rectangles decomposition. The numerical results are listed in Tables 1 and 2. Moreover, as to report the features of the block-centered finite difference method vividly, Figs. 1, 2, 3 and 4 are given with $N = 20, \ t = 0.5$ for Example 1. And in Example 2, set $\Omega = (-1, 1) \times (-1, 1)$. The initial spatial partition is a 5×5 grid. Then the grid is refined by dividing each edge into two equal parts and the nonuniform meshes are used which are generated from the corresponding uniform mesh by adding a random in both x and y directions (cf. Fig. 5). The numerical results are listed in Tables 3 and 4.

Table 1 Error and convergence rates of Example 1 on uniform grids

$N_x \times N_y$	$\|Z - p\|_{L^\infty(L^2)}$	$Order$	$\|\mathbf{W} - \mathbf{u}\|_{L^\infty(L^2)}$	Order	$\|\psi - c_f\|_{L^\infty(L^2)}$	$Order$
5 × 5	1.09E−2	–	1.72E−2	–	8.41E−5	–
10 × 10	2.84E−3	1.97	4.45E−3	1.95	2.18E−5	1.95
20 × 20	7.06E−4	2.01	1.11E−3	2.00	5.33E−6	2.03
40 × 40	1.76E−4	2.00	2.78E−4	2.00	1.32E−6	2.01
80 × 80	4.41E−5	2.00	6.94E−5	2.00	3.30E−7	2.00

Table 2 Error and convergence rates of Example 1 on uniform grids

$N_x \times N_y$	$\|\mathbf{Q} - \mathbf{q}\|_{L^\infty(L^2)}$	$Order$	$\|\mathbf{Q} - \mathbf{q}\|_{L^2(L^2)}$	Order	$\|\Theta - \phi\|_{L^\infty(L^2)}$	$Order$
5 × 5	5.06E−6	–	1.67E−6	–	3.74E−7	–
10 × 10	1.51E−6	1.82	4.72E−7	1.74	9.75E−8	1.94
20 × 20	3.83E−7	2.00	1.18E−7	1.98	2.42E−8	2.01
40 × 40	9.59E−8	2.00	2.94E−8	2.00	6.04E−9	2.00
80 × 80	2.40E−8	2.00	7.35E−9	2.00	1.51E−9	2.00

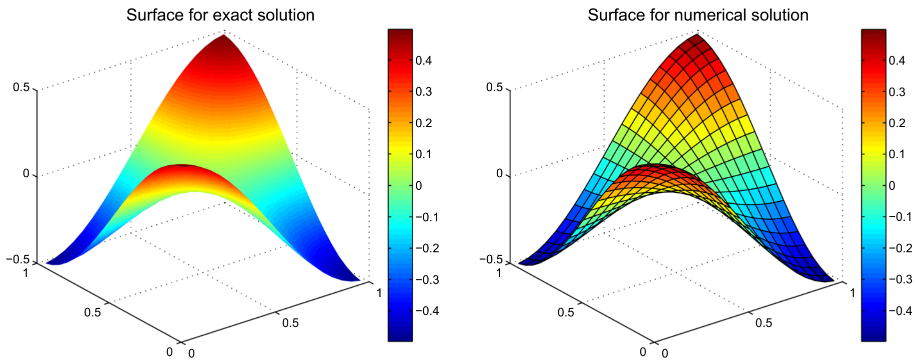

Fig. 1 The pressure figures for Example 1. *Left* the exact solution p. *Right* the numerical solution Z

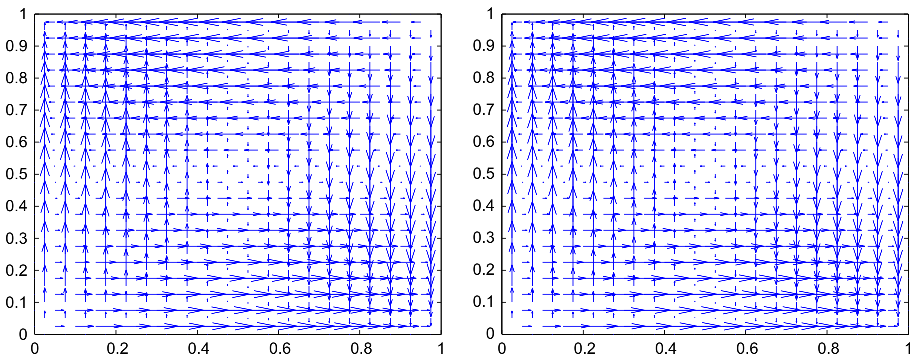

Fig. 2 The velocity figures for Example 1. *Left* the exact solution $\mathbf{u}$. *Right* the numerical solution $\mathbf{W}$

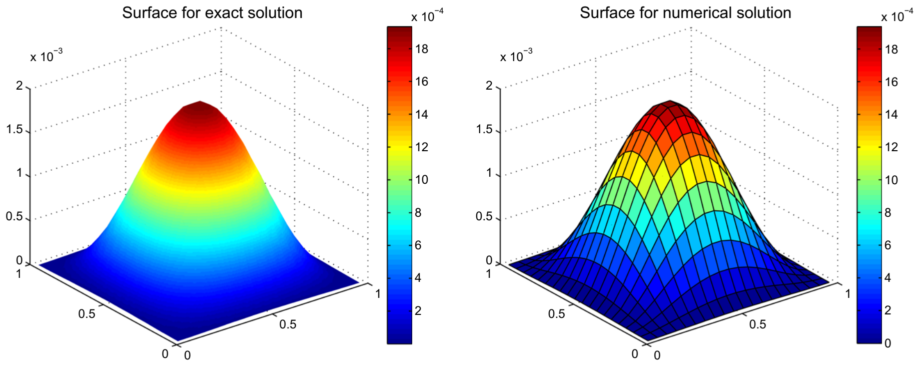

Fig. 3 The concentration figures for Example 1. *Left* the exact solution c_f. *Right* the numerical solution Ψ

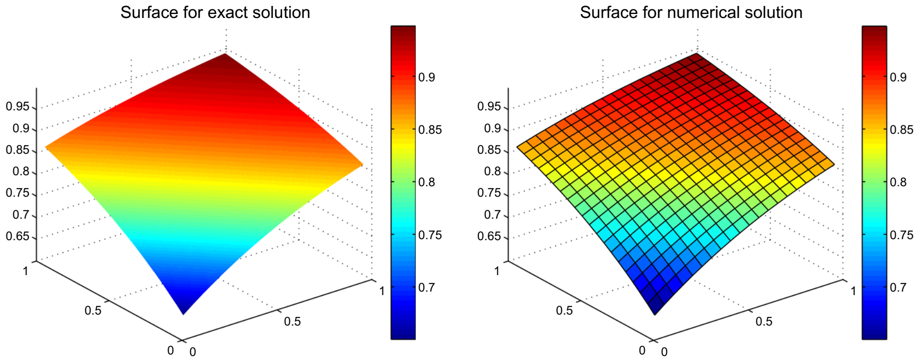

Fig. 4 The porosity figures for Example 1. *Left* the exact solution ϕ. *Right* the numerical solution Θ

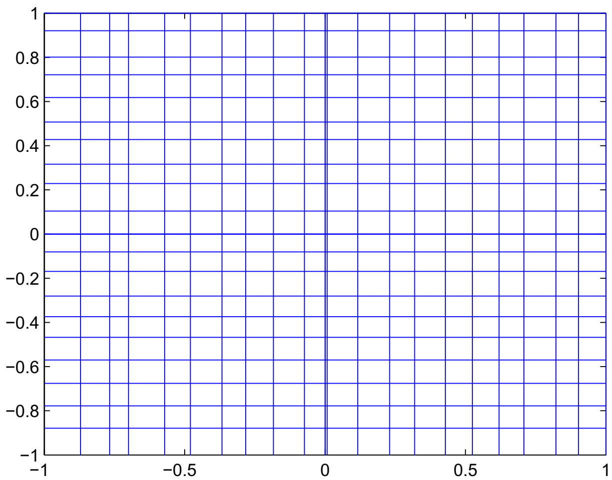

Fig. 5 The non-uniform mesh generated from the 20×20 uniform mesh for Example 2

Table 3 Error and convergence rates of Example 2 on nonuniform grids

$N_x \times N_y$	$\|Z-p\|_{L^\infty(L^2)}$	$Order$	$\|\mathbf{W}-\mathbf{u}\|_{L^\infty(L^2)}$	Order	$\|\psi-c_f\|_{L^\infty(L^2)}$	$Order$
5×5	7.42E−1	–	8.29E−2	–	2.22E−2	–
10×10	1.45E−1	2.36	2.46E−2	1.75	5.27E−3	2.08
20×20	3.75E−2	1.95	6.70E−3	1.88	1.52E−3	1.79
40×40	9.23E−3	2.02	1.71E−3	1.97	3.80E−4	2.00
80×80	2.30E−3	2.00	4.30E−4	1.99	9.49E−5	2.00

Table 4 Error and convergence rates of Example 2 on nonuniform grids

$N_x \times N_y$	$\|\mathbf{Q}-\mathbf{q}\|_{L^\infty(L^2)}$	$Order$	$\|\mathbf{Q}-\mathbf{q}\|_{L^2(L^2)}$	Order	$\|\Theta-\phi\|_{L^\infty(L^2)}$	$Order$
5×5	3.73E−4	—	1.64E−4	–	2.00E−3	–
10×10	1.13E−4	2.12	3.76E−5	1.73	5.00E−4	2.00
20×20	3.22E−5	1.81	1.02E−5	1.88	1.29E−4	1.95
40×40	8.07E−6	2.00	2.58E−6	1.98	3.23E−5	2.00
80×80	1.94E−6	2.06	5.87E−7	2.14	8.07E−6	2.00

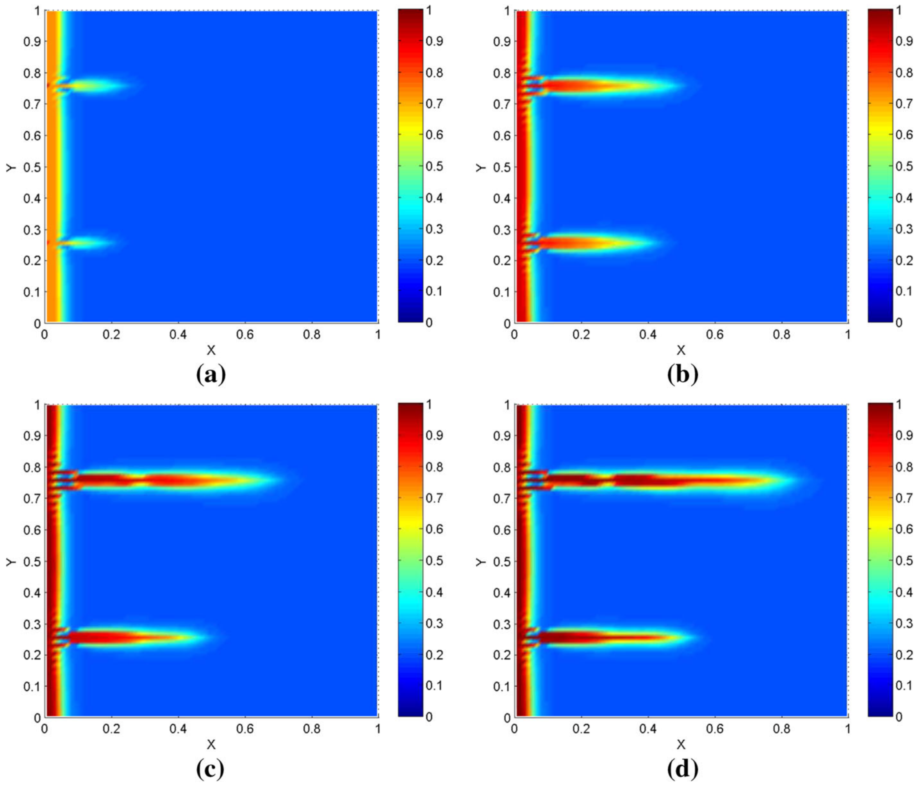

Fig. 6 The distributions of porosity for Example 3. **a** time $= 5\times10^5$ s, **b** time $= 1\times10^6$ s, **c** time $= 1.5\times10^6$ s, **d** time $= 2\times10^6$ s

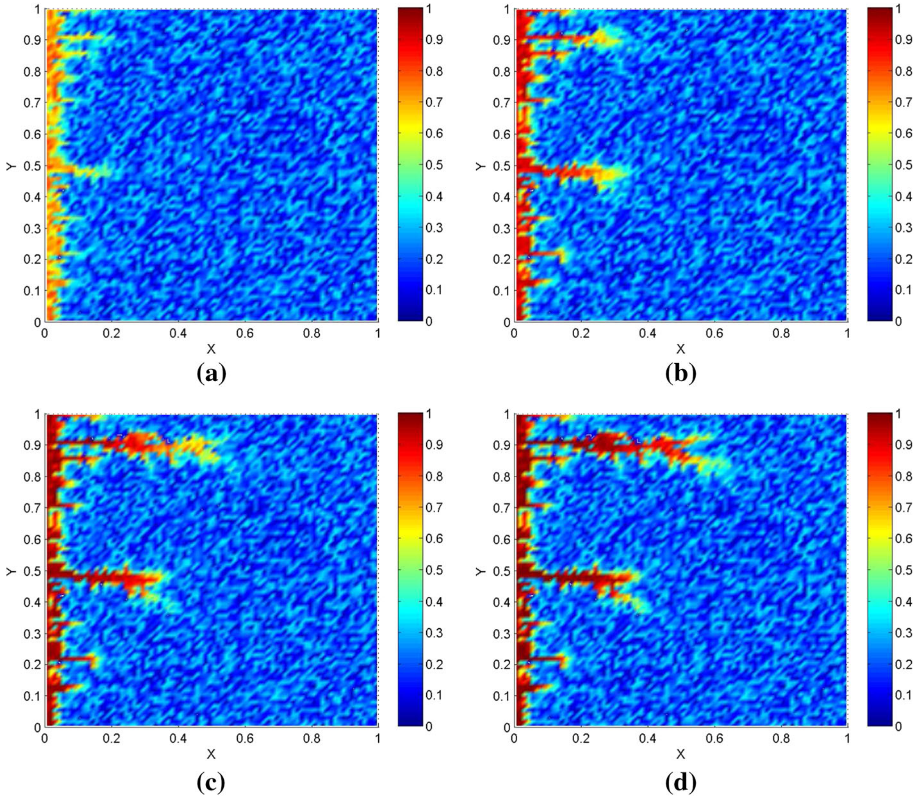

Fig. 7 The distributions of porosity for Example 4. **a** time $= 5\times10^5$ s, **b** time $= 1\times10^6$ s, **c** time $= 1.5\times10^6$ s, **d** time $= 2\times10^6$ s

Example 1 Here the initial condition and the right hand side of the equation are computed according to the analytic solution given as below.

$$\begin{cases} p(\mathbf{x},t) = tcos(\pi x)cos(\pi y), \\ c_f(\mathbf{x},t) = tx^2(1-x)^2y^2(1-y)^2, \\ \phi(\mathbf{x},t) = 1 - e^{-\frac{1}{80}t^2x^2(1-x)^2y^2(1-y)^2e^{x+y+1}-(x+y+1)}. \end{cases}$$

Example 2 Here the initial condition and the right hand side of the equation are computed according to the analytic solution given as below.

$$\begin{cases} p(\mathbf{x},t) = t(x+1)^2(x-1)^2(y+1)^2(y-1)^2, \\ c_f(\mathbf{x},t) = t\left(sin(\frac{\pi x}{2})sin(\frac{\pi y}{2})+1\right), \\ \phi(\mathbf{x},t) = 1 - e^{-\frac{1}{80}t^2(sin(\frac{\pi x}{2})sin(\frac{\pi y}{2})+1)e^{x+y+3}-(x+y+3)}. \end{cases}$$

In the following examples, $\Omega = (0,1)\times(0,1)$, $J = [0, 2\times10^6]$, $\Delta t = 2\times10^4$. the physical parameter is more realistic which is taken from the data in [1,3]. The the initial concentration of acid flow is zero. The initial pressure is 10^5 Pa. The parameter γ is set to 0.01. Besides, some properties of acid flow in porous media, the injection and production flow rates are listed as follows:

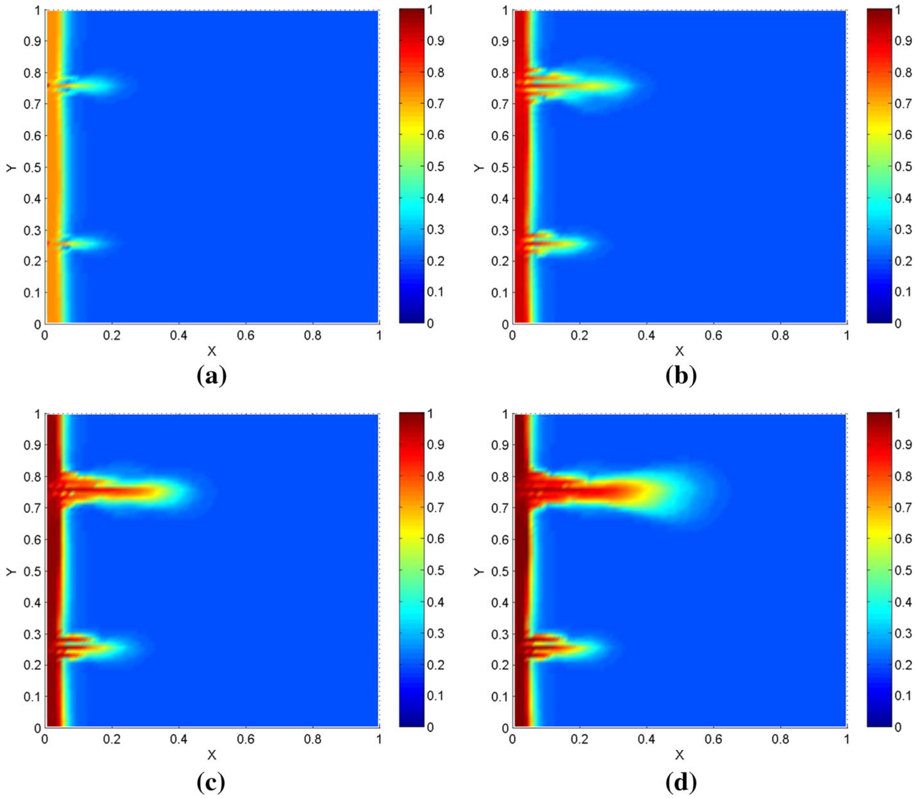

Fig. 8 The distributions of porosity for Example 5. **a** time $= 5\times10^5$ s, **b** time $= 1\times10^6$ s, **c** time $= 1.5\times10^6$ s, **d** time $= 2\times10^6$ s

$$\begin{cases} \mu = 10^{-2}, & \rho_s = 2500, \quad a_0 = 0.5, \\ \alpha = k_c = 0.1, & c_I = 10, \quad k_s = 1. \end{cases}$$

$$f_I = \begin{cases} 1, & x = 1/160, \\ 0, & otherwise. \end{cases} \quad f_P = \begin{cases} -1, & x = 159/160, \\ 0, & otherwise. \end{cases}$$

Example 3 In this example, $\mathbf{D} = 10^{-9}\,\mathbf{I}$. The distributions of initial porosity and permeability are listed as follows:

$$\begin{cases} \phi_0 = 0.4, & K_0 = 10^{-6}, & (x, y) = (1/160, 41/160), \\ \phi_0 = 0.6, & K_0 = 10^{-5}, & (x, y) = (1/160, 121/160), \\ \phi_0 = 0.2, & K_0 = 10^{-7}, & otherwise. \end{cases}$$

Example 4 In this example, $\mathbf{D} = 10^{-9}\,\mathbf{I}$. The initial porosity in the porous medium also obeys the uniform distribution and the range is from 0.05 to 0.35. The initial permeability of the porous media comply with the uniform distribution and the range is from 10^{-5} to 10^{-4}.

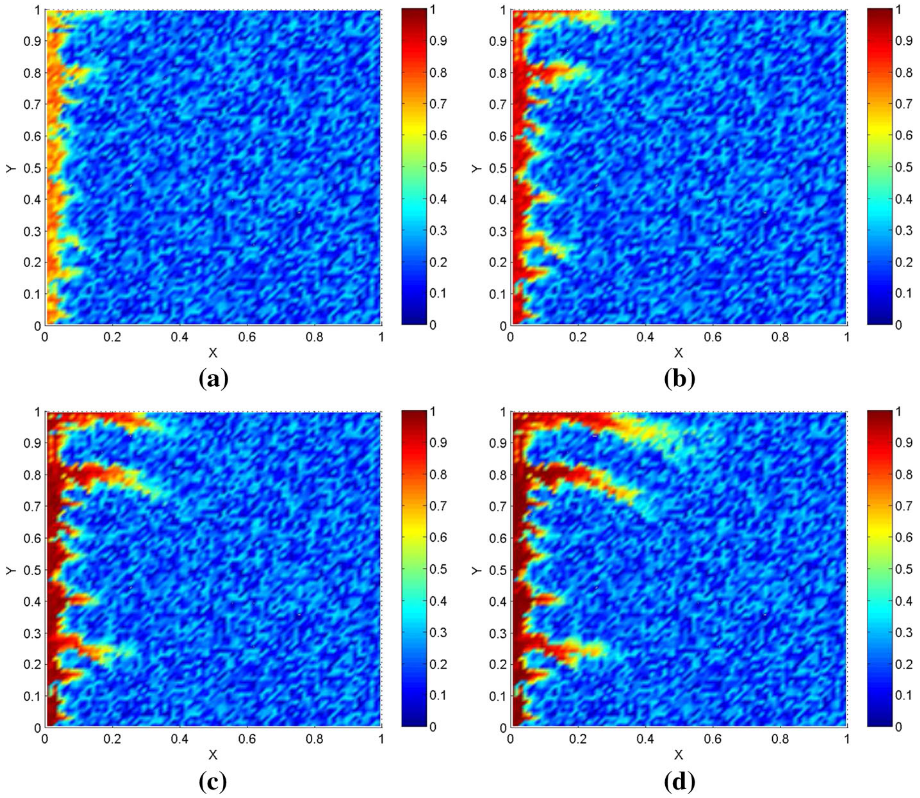

Fig. 9 The distributions of porosity for Example 6. **a** time = 5×10^5 s, **b** time = 1×10^6 s, **c** time = 1.5×10^6 s, **d** time = 2×10^6 s

Example 5 In this example, $d_m = 10^{-9}$, $\alpha_l = 10^{-3}$, $\alpha_t = 10^{-4}$. The distributions of initial porosity and permeability are listed as follows:

$$\begin{cases} \phi_0 = 0.4, & K_0 = 10^{-6}, \quad (x, y) = (1/160, 41/160), \\ \phi_0 = 0.6, & K_0 = 10^{-5}, \quad (x, y) = (1/160, 121/160), \\ \phi_0 = 0.2, & K_0 = 10^{-7}, \quad otherwise. \end{cases}$$

Example 6 In this example, $d_m = 10^{-9}$, $\alpha_l = 10^{-3}$, $\alpha_t = 10^{-4}$. The initial porosity in the porous medium also obeys the uniform distribution and the range is from 0.05 to 0.35. The initial permeability of the porous media comply with the uniform distribution and the range is from 10^{-5} to 10^{-4}.

The distributions of porosity for Examples 3–6 are calculated at the end of 25th time step, 50th time step, 75th time step and 100th time step respectively. We show the distributions of porosity in Figs. 6, 7, 8 and 9. These results are computed on the grid of 80 × 80 cells.

From Figs. 6, 7, 8 and 9, we can see that the average porosities in all frameworks are increasing, which reveal that the matrix is eaten by the acid. Moreover, it can be observed that at the beginning of the development, all frameworks demonstrate the formation of some small fingers. As time elapses, some major fingers appear. However, compared Figs. 6 and 7 with 8 and 9, we can see that the framework curves are thinner when the effective dispersion tensor D_e is diagonal.

From Tables 1, 2, 3 and 4 and Figs. 1, 2, 3, 4, 5, 6, 7, 8 and 9, we can see that the block-centered finite difference approximations for the pressure, velocity, porosity, concentration and its flux have the $(h^2 + \Delta t)$ accuracy in discrete norms. These results are in consistent with the error estimates in Theorem 9. As shown in Figs. 6, 7, 8 and 9, the heterogeneity of porosity and permeability in wormhole formations also has great effect on the field, which promotes the non-uniformity of the chemical reaction. Those examples vividly show that the block-centered finite difference method is capable of effectively simulating wormhole propagation.

7 Conclusion

In this paper, we have developed a block-centered finite difference method for compressible wormhole propagation during reactive dissolution of carbonate, which is effectively applied to enhance oil and gas production rate. The coupled analysis approach to deal with the fully coupling relation of multivariables is employed. Based on this method, stability analysis are established rigorously and carefully. Using estimates of the mixed finite element method with quadrature applied to linear parabolic equations, we obtain superconvergence of the pressure, velocity, porosity, concentration and its flux in different discrete norms on non-uniform grids. Finally, some numerical experiments are presented to verify the theoretical analysis and effectiveness of the given scheme.

Acknowledgements The authors would like to thank the editor and referees for their valuable comments and suggestions which helped us to improve the results of this paper. This work is supported by the National Natural Science Foundation of China Grant No. 11671233, the Science Challenge Project No. JCKY2016212A502.

References

1. Kou, J., Sun, S., Wu, Y.: Mixed finite element-based fully conservative methods for simulating wormhole propagation. Comput. Methods Appl. Mech. Eng. **298**, 279–302 (2016)
2. Panga, M.K., Ziauddin, M., Balakotaiah, V.: Two-scale continuum model for simulation of wormholes in carbonate acidization. AIChE J. **51**, 3231–3248 (2005)
3. Wu, Y., Salama, A., Sun, S.: Parallel simulation of wormhole propagation with the Darcy–Brinkman–Forchheimer framework. Comput. Geotech. **69**, 564–577 (2015)
4. Fredd, C.N., Fogler, H.S.: Influence of transport and reaction on wormhole formation in porous media. AIChE J. **44**, 1933–1949 (1998)
5. Golfier, F., Zarcone, C., Bazin, B., Lenormand, R., Lasseux, D., Quintard, M.: On the ability of a Darcy-scale model to capture wormhole formation during the dissolution of a porous medium. J. Fluid Mech. **457**, 213–254 (2002)
6. Liu, M., Zhang, S., Mou, J., Zhou, F.: Wormhole propagation behavior under reservoir condition in carbonate acidizing. Transp. Porous Media **96**, 203–220 (2013)
7. Zhao, C., Hobbs, B., Hornby, P., Ord, A., Peng, S., Liu, L.: Theoretical and numerical analyses of chemical-dissolution front instability in fluid-saturated porous rocks. Int. J. Numer. Anal. Methods Geomech. **32**, 1107–1130 (2008)
8. Li, X., Rui, H.: Characteristic block-centered finite difference method for simulating incompressible wormhole propagation. Comput. Math. Appl. **73**, 2171–2190 (2017)
9. Raviart, P.-A., Thomas, J.-M.: A Mixed Finite Element Method for 2-nd Order Elliptic Problems. Springer, Berlin (1977)
10. Arbogast, T., Wheeler, M.F., Yotov, I.: Mixed finite elements for elliptic problems with tensor coefficients as cell-centered finite differences. SIAM J. Numer. Anal. **34**, 828–852 (1997)

11. Rui, H., Pan, H.: A Block-centered finite difference method for the Darcy–Forchheimer model. SIAM J. Numer. Anal. **50**, 2612–2631 (2012)
12. Li, X., Rui, H.: Characteristic block-centred finite difference methods for nonlinear convection-dominated diffusion equation. Int. J. Comput. Math. **94**, 384–404 (2015)
13. Li, X., Rui, H.: A two-grid block-centered finite difference method for nonlinear non-Fickian flow model. Appl. Math. Comput. **281**, 300–313 (2016)
14. Rui, H., Pan, H.: Block-centered finite difference methods for parabolic equation with time-dependent coefficient. Japan J. Ind. Appl. Math. **30**, 681–699 (2013)
15. Rui, H., Liu, W.: A two-grid block-centered finite difference method for Darcy–Forchheimer flow in porous media. SIAM J. Numer. Anal. **53**, 1941–1962 (2015)
16. Liu, Z., Li, X.: A parallel CGS block-centered finite difference method for a nonlinear time-fractional parabolic equation. Comput. Methods Appl. Mech. Eng. **308**, 330–348 (2016)
17. Li, X., Rui, H.: A two-grid block-centered finite difference method for the nonlinear time-fractional parabolic equation. J. Sci. Comput. (2017). doi:10.1007/s10915-017-0380-4
18. Mauran, S., Rigaud, L., Coudevylle, O.: Application of the Carman–Kozeny correlation to a high-porosity and anisotropic consolidated medium: the compressed expanded natural graphite. Transp. Porous Media **43**, 355–376 (2001)
19. Nédélec, J.-C.: Mixed finite elements in $\mathbb{R}$ 3. Numer. Math. **35**, 315–341 (1980)
20. Weiser, A., Wheeler, M.F.: On convergence of block-centered finite differences for elliptic problems. SIAM J. Numer. Anal. **25**, 351–375 (1988)
21. Dawson, C.N., Wheeler, M.F., Woodward, C.S.: A two-grid finite difference scheme for nonlinear parabolic equations. SIAM J. Numer. Anal. **35**, 435–452 (1998)
22. Durán, R.: Superconvergence for rectangular mixed finite elements. Numer. Math. **58**, 287–298 (1990)
23. Douglas, J., Roberts, J.E.: Numerical methods for a model for compressible miscible displacement in porous media. Math. Comput. **41**, 441–459 (1983)
24. Guo, Q., Zhang, J.Wang: Error analysis of the semi-discrete local discontinuous Galerkin method for compressible miscible displacement problem in porous media. Appl. Math. Comput. **259**, 88–105 (2015)